Coexistence of Thread and Sheet Chaotic Attractors for Three Dimensional Lozi Map

René LOZI *

Posted Date: 11 May 2023

doi: 10.20944/preprints202305.0775.v1

Keywords: chaotic attractor; hyperchaotic attractor; Lozi map; sheet-attractor; thread-attractor

Article

Coexistence of Thread and Sheet Chaotic Attractors for Three Dimensional Lozi Map

René Lozi

LJAD, CNRS, Université Côte d'Azur, F-06000 Nice, France; rene.lozi@univ-cotedazur.fr

Abstract: Since its original publication in 1978, Lozi's chaotic map has been thoroughly explored and continues to be. Hundreds of publications analyze its particular structure or apply its properties in many fields (electronic devices like memristor, A.I. with swarm intelligence, etc.). Several generalizations have been proposed, transforming the initial two-dimensional map into multidimensional one. However, they do not respect the original constraint that allows this map to be one of the few strictly hyperbolic: a constant Jacobian. In this paper we introduce a three-dimensional piece-wise linear extension respecting this constraint and we explore a special property never highlighted for chaotic mappings: the coexistence of *thread*-chaotic attractors (i.e., attractors which are formed by collection of lines) and *sheet*-chaotic attractors (i.e., attractors which are formed by collection of planes). This new 3-dimensional mapping can generate a large variety of chaotic and hyperchaotic attractors. We give five examples of such behavior in this article. In the first three examples, there is coexistence of *thread* and *sheet*-chaotic attractors. However, their shape are different and they are constituted by a different number of pieces. In the two last examples, the blow up of the attractors with respect to parameter a and b is highlighted.

Keywords: Lozi map; strange attractors; sheet hyperchaotic attractors; thread chaotic attractors; blow up of attractor

1. Introduction

Since its original publication in 1978, Lozi's chaotic map has been thoroughly explored and continues to be. Hundreds of publications analyze its particular structure or apply its properties in many fields (cryptography, optimization, secure communications, electronic devices like memristor, A.I. with swarm intelligence, etc.). Several kinds of generalization have been proposed, transforming the initial two-dimensional map into multidimensional. However, they do not respect the original constraint that allows this map to be one of the few strictly hyperbolic: a constant Jacobian. In this paper we introduce a three-dimensional piece-wise linear extension respecting this constraint and we explore a special property never highlighted for chaotic mappings: the coexistence of *thread-chaotic attractors* (i.e., attractors which are formed by collection of lines) and *sheet-hyperchaotic attractors* which are formed by collection of planes).

In Section 2, we recall the history and initial defin(i.e., attractorsition of the Lozi map, its chaotic properties in the dissipative case, the dynamics features (fixed points, invariant manifolds, basin of attraction, etc.). We describe also the chaotic properties in the conservative case. We do a rapid survey of the generalization of such map: topological generalizations (*Lozi-like* map), geometrical generalization (*Lozi-type* map), generalization of the formula in dimension 3 or more, fractal generalization, non-conventional generalization and networks of Lozi maps with chimera. In Section 3 we recall the definition of two Rössler hyperchaotic attractors for comparison, and we introduce a new generalization fo the Lozi map in three dimensions. In Section 4 we give the basic properties of the *thread* and *sheet*-attractors (fixed point, period-two orbit). This new 3-dimensional mapping can generate a large variety of chaotic and hyperchaotic attractors. We give five examples of such behavior in this section. In the first three examples, there is coexistence of *thread* and *sheet* chaotic attractors. However, their shape are different and they are constituted by a different number of pieces. In the two last examples,

Preprints (www.preprints.org) | NOT PEER-REVIEWED | Posted: 11 May 2023 doi:10.20944/preprints202305.0775.v1

the blow up of the attractors with respect to parameter a and b is highlighted. A brief conclusion is drawn in Section 5.

2. The Lozi map

2.1. History

The Lozi map was found by René Lozi exactly on 15 June 1977 around 11 am during the defense of the Ph. D. thesis of one of his colleague in the department of mathematics of the University of Nice (France) [1] (p. xxv).
As he explained in [2], the week before, he attended the International Conference on Mathematical Problems in Theoretical Physics in Roma. The opening talk was given by David Ruelle on 6 June, who conjectured in his presentation that, for the Hénon attractor, the theoretical entropy should be equal to the characteristic exponent [3]. This is how he discovered the first example of chaotic and strange attractors (See Figure 1).

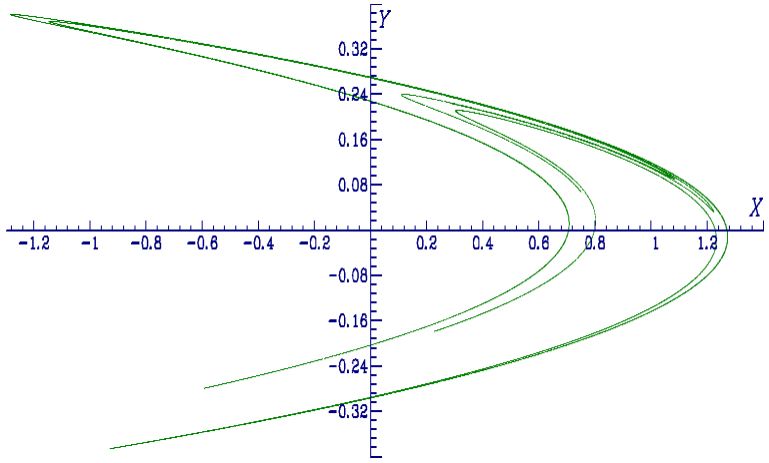

Figure 1. Hénon map, for the parameter value $a = 1.4$, $b = 0.3$, initial value $x_0 = 0$, $y_0 = 0$.

Hénon who explored numerically the Lorenz map [4] using a IBM-7040 found it difficult to highlight its inner nature due to its very strong dissipativity. Its rate of volume contraction is given by the Lie derivative of the Lorenz equations which can be solved. For the parameters chosen by Lorenz, $V(t) = V(0)e^{\frac{-41}{3}}$. Therefore, after one time unit, volumes are reduced by a factor 10^6. Inspired by his astronomer experience of Poincaré's map for the motion of planets, Hénon built the metaphoric model [5]

$$\begin{cases} x_{n+1} = 1 - ax_n^2 + y_n, \\ y_{n+1} = bx_n, \end{cases} \tag{1}$$

also represented by the iterates of any initial point $(x_0, y_0)^T$ by the map $\mathcal{H}_{a,b} : \mathbb{R}^2 \longrightarrow \mathbb{R}^2$

$$\mathcal{H}_{a,b} \begin{pmatrix} x \\ y \end{pmatrix} = \begin{pmatrix} 1 - ax^2 + y, \\ bx. \end{pmatrix} \tag{2}$$

For this map the contracting properties are only determined by the parameter b. With $b = 0.3$, the contraction in one iteration is mild enough that the sheaves of the attractors are visible. Eventually he observed graphically the fractal structure of the attractor which astonished the research community.

Preprints (www.preprints.org) | NOT PEER-REVIEWED | Posted: 11 May 2023 doi:10.20944/preprints202305.0775.v1

2.1.1. Initial definition

At this time, Lozi was working in numerical analysis, in the domain of bifurcation which was not very developed in France. His main interest was focused on discretization problem and finite element method in which nonlinear functions are approximated by piecewise linear ones. During the Roma conference, he tried unsuccessfully to apply the spirit of the method of finite element to the Hénon attractor. Back to Nice after this conference, he eventually decided, using paper and pencil, to change the square function of the Hénon attractor, which is U shaped, into the absolute value function, which has a V shape, implying folding property (folding property is important for horseshoe a main ingredient of chaos, as highlighted by Stephen Smale [6]).
He tested this modification, on a small desktop computer HP 9820 linked to a HP 9862 plotter and found a similar attractor of the Hénon attractor, with straight lines instead of curves for the map [7] (See Figure 2).

$$\mathcal{L}_{a,b}\begin{pmatrix} x \\ y \end{pmatrix} = \begin{pmatrix} 1 - a\,|x| + y, \\ bx. \end{pmatrix} \tag{3}$$

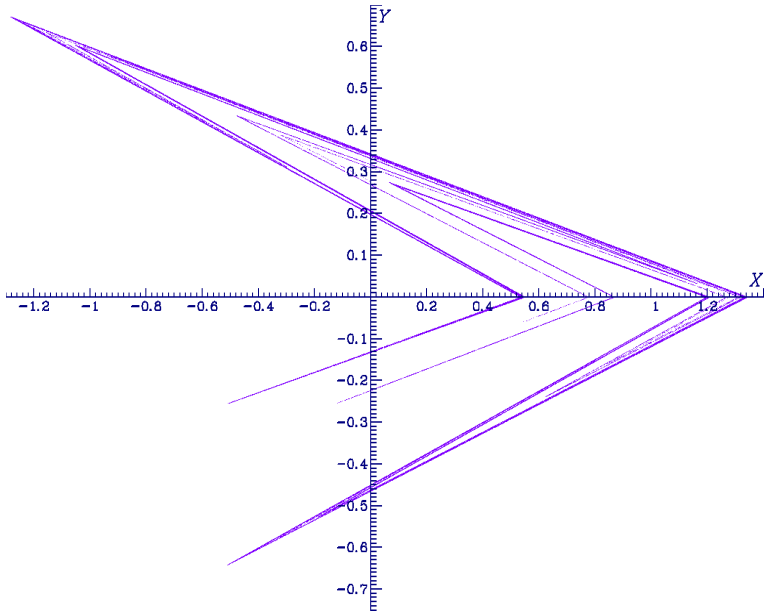

Figure 2. Original Lozi map in dimension 2 for the parameter value $a = 1.7, b = 0.5$, initial value $x_0 = 0, y_0 = 0$.

2.1.2. Chaotic properties of the dissipative map (|b|<1)

When $|b| < 1$ the map is called "dissipative" that means that the image of any subset Δ by f has a measure which is less than the measure of Δ : $measure(f(\Delta)) < measure(\Delta)$.

Two years after the discovery of this new chaotic attractor and only one year after its publication [7], at the end of 1979, during the *International Conference on Nonlinear Dynamics*, patronized by the New-York Academy of Sciences on December 17-21, 1979, Michal Misiurewicz, presented a rigorous proof that for a set of parameters $\mathcal{S}$ this map has a strange attractor, coining at this occasion the name 'Lozi map' [8]. This set in the plane of parameters (a, b) is defined by (See Figure 3).

$$\mathcal{S} = \left\{ (a,b) \,\middle|\, b > 0, a\sqrt{2} < b + 2, b < \frac{a^2 - 1}{2a + 1}, 2a + b < 4 \right\} \tag{4}$$

Preprints (www.preprints.org) | NOT PEER-REVIEWED | Posted: 11 May 2023 doi:10.20944/preprints202305.0775.v1

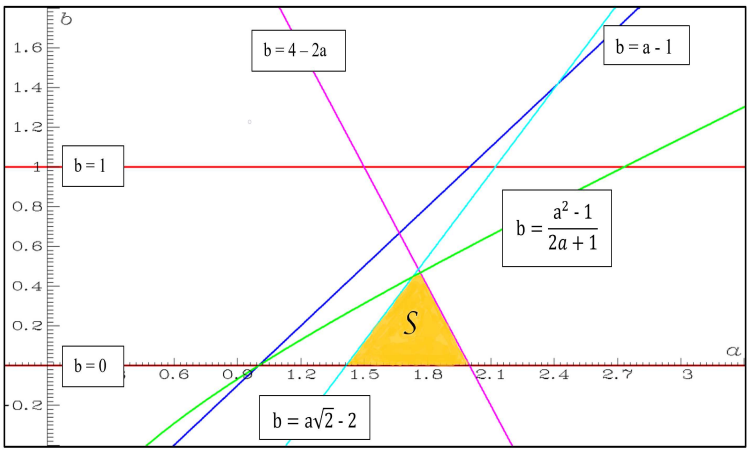

Figure 3. The set $\mathcal{S}$ of the plane of parameters where Lozi map has a strange attractor in the first proof of Misiurewicz [8]. Red lines $b = 0$ and $b = 1$, blue line $b = a - 1$, pink line $b = -2a + 4$, cyan line $b = a\sqrt{2} - 2$, green curve $b = \frac{a^2-1}{2a+1}$.

This set of parameter $\mathcal{S}$ (defined only for $b > 0$) was later slighty enlarged (as $\mathcal{S}^+$ in Figure 4) in the upper edge of the triangle by Misiurewicz and Stimac [9], removing the condition $b < \frac{a^2-1}{2a+1}$.

$$\mathcal{S}^+ = \left\{(a,b) \,\middle|\, b > 0, a\sqrt{2} < b + 2, 2a + b < 4\right\} \tag{5}$$

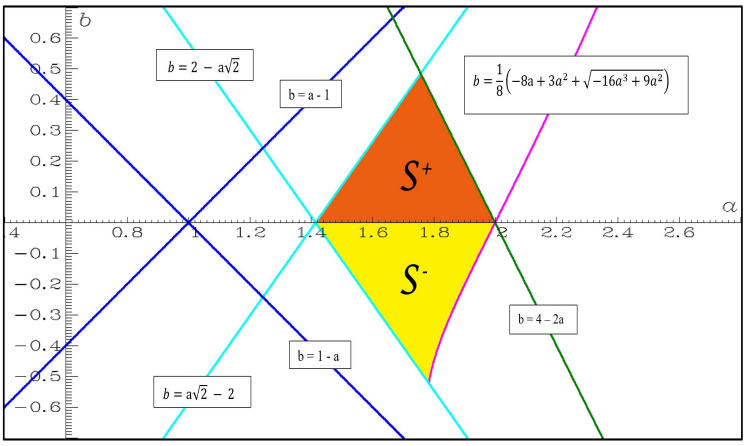

Figure 4. The sets $\mathcal{S}^+$ and $\mathcal{S}^-$ of the plane of parameters where Lozi map has a strange attractor in the second proof of Misiurewicz and Stimac [9] and the proof of Kucharski [10]. Blue lines $b = a - 1$ and $b = 1 - a$, cyan lines $b = a\sqrt{2} - 2$ and $b = 2 - a\sqrt{2}$, green line $b = 4 - 2a$, pink line $b = \frac{-8a+3a^2+\sqrt{-16a^3+9a^4}}{8}$.

Recently the case $b < 0$ was studied by Kucharski [10], who found a quasi-symmetric set of parameters $\mathcal{S}^-$ (Figure 4) however, not completely symmetric for the right handside boundary.

$$\mathcal{S}^- = \left\{(a,b) \,\middle|\, -1 < b < 0, a\sqrt{2} > b + 2, b > \frac{-8a + 3a^2 + \sqrt{-16a^3 + 9a^4}}{8}\right\} \tag{6}$$

2.1.3. Fixed points, invariant manifolds and basin of attraction

Due to the piecewise linearity of absolute value in $\mathcal{L}_{a,b}$ (3), one can compute explicitly the fixed points and the periodic orbit of any order of it.

Preprints (www.preprints.org) | NOT PEER-REVIEWED | Posted: 11 May 2023 doi:10.20944/preprints202305.0775.v1

When $1-a < b < a+1$ (for $a > 0$ both regions $\mathcal{S}^-$ and $\mathcal{S}^+$ are in the cone defined by theses inequalities), there exist two fixed points

$$\mathcal{A} = \left(\frac{1}{a+1-b}, \frac{b}{a+1-b} \right),$$

which belongs to the quadrant $\{x \geq 0, y \geq 0\}$, and

$$\mathcal{B} = \left(\frac{1}{1-a-b}, \frac{b}{1-a-b} \right),$$

which belongs to the quadrant $\{x < 0, y < 0\}$.

Furthermore, one can easily compute the local stability of these points by evaluating the corresponding eigenvalues of the Jacobian matrix of $\mathcal{L}_{a,b}$, and conclude that, in the domain of the parameter space where both $\mathcal{A}$ and $\mathcal{B}$ coexist, that is, for $a > |b| + 1$, they are saddle points.
Interestingly, the chaotic attractor of the Lozi map belongs to the unstable invariant manifold of $\mathcal{A}$. More exactly from [8] it is known that the chaotic (and strange) attractor $\tilde{\mathcal{F}}$ can be constructed from the successive forward iterations of a trapping region F,

$$\tilde{\mathcal{F}} = \bigcap_{n=0}^{\infty} \mathcal{L}^n(F),$$

with F the triangle with vertices at the points I, $\mathcal{L}(I)$, and $\mathcal{L}^2(I)$, where I is the point given by the intersection of the unstable manifold of the fixed point $\mathcal{A}$ with the horizontal axis,

$$I = \left(\frac{2+a+\sqrt{a^2+4b}}{2(1+a-b)}, 0 \right).$$

Baptista et al. [11] have found that the basin of attractor is modeled by some parts of the stable manifold of the fixed point $\mathcal{B}$. They consider the point X intersection of this stable manifold with the vertical axis. A simple computation gives its expression as

$$X = \left(0, \frac{b(2-a+\sqrt{a^2+4b}}{(a-\sqrt{a^2+4b})(a+b-1)} \right).$$

and a certain point T belonging on the horizontal axis, first defined by Ishii [12] whose expression is

$$X = \left(\frac{b(2-a+\sqrt{a^2+4b}(a(1+b)+(1-b)\sqrt{a^2+4b})}{(1-a-b)(a-\sqrt{a^2+4b})(a-\sqrt{a^2+4b})(2b(b-1)+a^2(1+2b)+a(1-2b)\sqrt{a^2+4b})}, 0 \right).$$

They show that the basin of attraction is bounded by a polygonal line entirely characterized by the points T, X and their successive preimages.

2.1.4. Other dynamical properties of the dissipative map (| b | <1)

Boroński, Kucharski and Ou [13] rigorously determined an open region in the parameter space for which Lozi map exhibits periodic points of least period n, for all $n > 13$.

$$\mathcal{P}_{str} = \{(a,b) \,|\, b > 0, b < l_{str}(a) \text{ when } a < a_0, \text{ and } b < l_{tan}(a) \text{ when } a > a_0\} \tag{7}$$

and

$$\mathcal{P}_3(a,b) = \left\{(a,b) \,|\, 0 \leq b \leq 1 \,,\, a > l_{hyp}(b), \text{ and } a > l_3(b)\right\} \tag{8}$$

Preprints (www.preprints.org) | NOT PEER-REVIEWED | Posted: 11 May 2023 doi:10.20944/preprints202305.0775.v1

where $a_0 = \frac{2}{7}\left(2+3\sqrt{2}\right) \approx 1.78$, $l_{str}(a) = -2+\sqrt{2}a$, $l_{tan}(a) = \frac{1}{8}\left(8a-3a^2-\sqrt{9a^4-16a^3}\right)$, $l_{hyp}(b) = b+1$,
and $l_3(b) = \frac{1}{2}\left[1-b+\sqrt{(1-b)^2+4(1-b+b^2)}\right]$.

Theorem 1 ([13]). *For all $(a,b) \in \mathcal{P}_{str} \cap \mathcal{P}_3$ the Lozi map $\mathcal{L}_{a,b}$ has a periodic point of least period n, for $n = 1,2,3$ and all $n > 13$.*

It is not in the scope of this article to provide a survey of all the papers describing the other dynamical or statistical properties of the Lozi map, because they are too numerous. One may refer to [1] for a compendium of results published between 1997 to 2013. Below, only some particular or more recent results are pointed out.

Many authors have published results on bifurcations of such map, like Botella-Soler et al. [14] showing that it presents what they call *bisecting bifurcations*: those which are mediated by an infinite set of neutrally stable periodic orbits.

Sushko et al. [15] investigate the bifurcation structure of the parameter plane in the vicinity of the curve related to a center bifurcation of the fixed point. A distinguishing property of the Lozi map is that it is conservative (see Section 2.1.5) at the parameter value corresponding to this bifurcation. As a result, the bifurcation structure close to the center bifurcation curve is quite complicated. In particular, an attracting fixed point (focus) can coexist with various attracting cycles, as well as with chaotic attractors, and the number of coexisting attractors increases as the parameter point approaches the center bifurcation curve. Their study contributes also to the border collision bifurcation theory since the Lozi map is a particular case of the 2D border collision normal form (2D-BCNF).

Glendinning and Simpson [16] use as canonical example the following 2D-BCNF which is the family of difference equations $(x,y) \longrightarrow f(x,y)$

$$f(x,y) = \begin{cases} A_L \begin{bmatrix} x \\ y \end{bmatrix} + \begin{bmatrix} \mu \\ 0 \end{bmatrix}, & x \leq 0, \\ A_R \begin{bmatrix} x \\ y \end{bmatrix} + \begin{bmatrix} \mu \\ 0 \end{bmatrix}, & x \geq 0, \end{cases} \tag{9}$$

and with

$$A_L = \begin{bmatrix} \tau_L & 1 \\ -\delta_L & 0 \end{bmatrix}, \quad A_R = \begin{bmatrix} \tau_R & 1 \\ -\delta_R & 0 \end{bmatrix}.$$

They restrict in their paper their attention to the parameter values $\tau_R \in \mathbb{R}$, $\tau_L > 0$, $\delta_L > 0$, $\delta_R > 0$, $\mu = 1$, for which f is invertible and orientation-preserving.

The role of μ is to control the border-collision bifurcation. In view of a linear rescaling, it is only needed to consider it for the values $\{-1,0,1\}$ (here it is 1). The condition $\tau_L > 0$ is needed for the definition of the induced map. If $\tau_L = -\tau_R$ and $\delta_L = \delta_L$ then the 2d BCNF reduces to the Lozi map.

In addition of bifurcation studies, Collet and Levy [17] consider ergodic properties of such mapping, that they consider as intermediate stage between the Axiom A dynamical systems and more complicated systems like the Hénon map. They construct its Bowen-Ruelle measure and also derive some of its properties which are similar to those of an axiom A system.

Rychlik [18] gives a proof of the existence of Sinai-Bowen-Ruelle measures (SBR measures) for this map. He also proves that the number of SBR measures is finite.
Cao and Liu [19] explore the geometric structure of its chaotic attractor and proof:

Preprints (www.preprints.org) | NOT PEER-REVIEWED | Posted: 11 May 2023 doi:10.20944/preprints202305.0775.v1

Proposition 1. *If the parameters* (a, b) *satisfy Misiurewicz conditions* (4)*, then the strange attractor* $\Lambda_{a,b}$ *possesses the following properties:*

- *The union of the transversal homoclinic points and weak transversal homoclinic points are dense in* $\Lambda_{a,b}$.
- *All periodic points are hyperbolic.*
- *The set of periodic points forms a dense set in* $\Lambda_{a,b}$.
- *Any two hyperbolic points forms a transversal heteroclinic cycle or a weak transversal heteroclinic cycle.*

Other statistical (hyperbolic, ergodic and topological) properties are described in Afraimovich et al. [20].

The symbolic dynamics of this map is also greatly studied. In 1991, Zheng [21] describes some details of it. Two families of symbolic sequences are assigned for two groups of lines in the phase plane, the order of symbolic sequences is defined, and the ordering rules derived. Misiurewicz and Stimac [9] in a more detailed study introduce the set of kneading sequences for this map and prove that it determines its symbolic dynamics. They also introduce two other equivalent approaches. One can cite also in this field of research, the important works of Ishii [12,22], Sand [23], and de Carvalho and Hall [24]. In [12], Ishii constructs a kneading theory à la Milnor-Thurston and shows that topological properties of the dynamics of the Lozi map are determined by its pruning front and primary pruned region only. This gives a solution to the first tangency problem for the Lozi family, moreover the boundary of the set of all horseshoes in the parameter space is shown to be algebraic. As an application of this result, in [22] the partial monotonicity of the topological entropy and of bifurcations near horseshoes is proved. Upper and lower bounds for the Hausdorff dimension of the Lozi attractor are also given in terms of parameters. In [24] recent results on pruning theory are given, concentrated on prunings of the horseshoe. in [23] the monotonicity of the Lozi family when the Jacobian determinant is close to zero is showed. The main ingredients of the proof therein are the 'pruning pair method' and a detailed analysis of the parameter dependence of the kneading invariant of the tent-map family.

2.1.5. Chaotic properties of the conservative map ($|b|=1$)

In the conservative case (also called area-preserving) $measure(f(\Delta)) = measure(\Delta)$, there is no attractor.

Li et al. [25] study this case and highlight that it can generate initial values-related coexisting infinite orbits. Its moving orbits are extremely dependent on its initial values and present periodic, quasi-periodic and chaotic orbits, with different types and topologies. In other words, the emergence of extreme multistability appears in the area-preserving Lozi map. As an example several of such orbits are plotted in (Figure 5). Li et al. note that the coexistence of double or multiple attractors has been found in the Hénon map, the M-dimensional nonlinear hyperchaotic model [26], and the multistage DC/DC switching converter [27]; that two types of simple 2D hyperchaotic maps with sine trigonometric nonlinearity and constant controllers were shown to generate initial-boosted infinite attractors along a phase line [28,29]. Recently, a simple two-dimensional Sine map was presented to obtain the initials-boosted infinitely many attractors along a phase plane [30]. However, they emphasize that all these newly presented discrete maps only exhibit the coexisting attractors with different positions. However, the coexisting infinite attractors with different topologies and different positions in the discrete maps are rarely reported like in the area-preserving Lozi Map.

In addition to the analysis of Sushko et al. [15] (see Section 2.1.4), this conservative map is also studied by Lopesino et al. in [31] who proof when $a > 4$, the existence of a chaotic saddle in the square

$$\mathcal{S}_q = \left\{ (x, y) \in \mathbb{R}^2 \mid |x| \leq R,\ |y| \leq R \right\}$$

with

$$R = R(a) = \frac{a}{4(a-2)}. \tag{10}$$

Preprints (www.preprints.org) | NOT PEER-REVIEWED | Posted: 11 May 2023 doi:10.20944/preprints202305.0775.v1

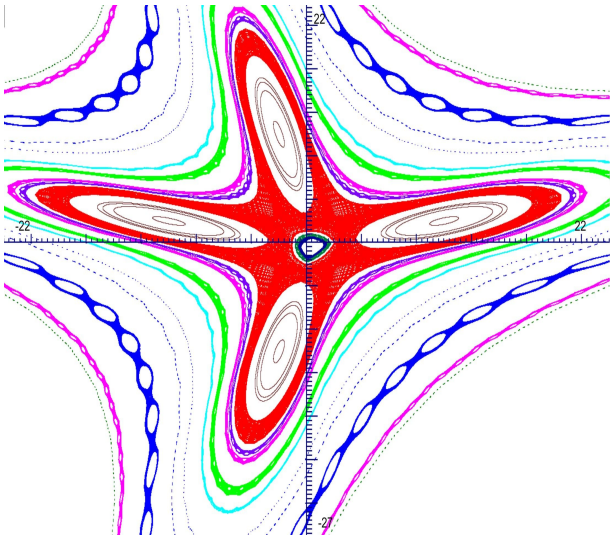

Figure 5. Periodic, quasi-periodic and chaotic orbits of the area-preserving map (3) in the plane (x, y) when $a = 0.5$ and $b = -1$. Initial values: red (most extended chaotic orbit) $x_0 = 1.3$, $y_0 = 2.0$, dark blue (innermost chaotic orbit inside the red orbit) $x_0 = 1.3$, $y_0 = -0.2$, dark green (chaotic orbit inside the red orbit); $x_0 = 1.7$, $y_0 = -0.2$ (chaotic orbit inside the red orbit); from $(10.0,\ 2.0)$ to upper right corner: brown (periodic orbit) $x_0 = 10.0$, $y_0 = 2.3$, brown (periodic orbit) $x_0 = 10.0$, $y_0 = 3.0$, brown (periodic orbit) $x_0 = 10.0$, $y_0 = 3.2$, brown (periodic orbit) $x_0 = 10.0$, $y_0 = 3.3$; from origin to upper right corner: purple (chaotic orbit) $x_0 = 10.0$, $y_0 = 4.6$, magenta (chaotic orbit) $x_0 = 10.0$, $y_0 = 5.0$, light green (chaotic orbit) $x_0 = 10.0$, $y_0 = 6.0$, light blue (chaotic orbit) $x_0 = 10.0$, $y_0 = 6.8$, dark blue (quasiperiodic orbit) $x_0 = 10.0$, $y_0 = 8.5$, dark blue (quasiperiodic orbit) $x_0 = 10.$, $y_0 = 9.6$, dark blue (chaotic orbit) $x_0 = 10.$, $y_0 = 13.0$, pink (chaotic orbit) $x_0 = 10.0$, $y_0 = 16.0$, green (quasiperiodic orbit) $x_0 = 10.0$, $y_0 = 17.0$.

2.2. Generalizations

A general trend in mathematics is to generalize any new mathematical object. Due to the simplicity of the equations defining the Lozi map (3), the simplest way to generalize it, is to increase the dimension of the discrete dynamical system associated adding similar equations. Another way is to generalize its topological or geometrical properties, and a recent third way is to define this map in the new paradigm of fractional mappings. Beside those ways, recently, a non-conventional generalization entangling this map with cosine and exponential functions has been proposed. Additionally, the Lozi map can be used to construct networks of chaotic attractors, either alone or with Hénon map.
It is the second way which was first explored in 1985 by Lai-Sang Young [32] who defined a *generalized Lozi map* (also called *Lozi-like map*) and later in 2018 by Misiurewicz and Stimac [33] who defined another kind of *Lozi-like map* without any reference or relationship with the definition of Young. Instead Juang and Chang [34] defined in 2010 a geometrical generalization called *Lozi-type map*.

2.2.1. Topological generalizations: *Lozi-like maps*

Let $\mathcal{R} = [0,1] \times [0,1]$ and let $f : \mathcal{R} \longrightarrow \mathcal{R}$ be a continuous injective map. Suppose that f (or some iterate of f) takes $\mathcal{R}$ into its interior.

Definition [32] A continuous injective map $f : \mathcal{R} \longrightarrow \mathcal{R}$ of $\mathcal{R} = [0,1] \times [0,1]$ is a *generalized Lozi map* if it satisfies the following conditions.

(L.1) There exist $0 < a_1 < \cdots < a_n < 1$ such that f is a $\mathcal{C}^1$-diffeomorphism on $\mathcal{R} \setminus \bigcup_{i=1}^{n} Y_i$ where $Y_i = \{a_i\} \times [0,1]$.
From now on, we set $\mathcal{S} = \bigcup_{i=1}^{n} Y_i$.
(L.2) The norm of the derivative Df of f is uniformly bounded on $\mathcal{R} \setminus \mathcal{S}$, i.e.,

Preprints (www.preprints.org) | NOT PEER-REVIEWED | Posted: 11 May 2023 doi:10.20944/preprints202305.0775.v1

$$M_f = sup\{\|Df_x\|; x \in \mathcal{R} \setminus \mathcal{S}\} < \infty,$$

where $\|Df_x\| = \sup\{\|Df_x(\mathbf{v})\|\}$; $\mathbf{v} \in T_x(\mathcal{R})$, $\|\mathbf{v}\| = 1$.

(L.3) There exist constants $|\lambda^s| < 1 < |\lambda^u|$ and continuous cone-fields $C^s = \{C^s_x\}_{x\in\mathcal{R}}$, $C^u = \{C^u_x\}_{x\in\mathcal{R}}$, on $\mathcal{R} \setminus \mathcal{S}$ and any vectors $\mathbf{x} \in \mathcal{R} \setminus \mathcal{S}$ and any vectors $\mathbf{v} \in C^u_x$, $\mathbf{w} \in C^s_{f(x)}$

- $Df_x\left(C^u_x\right) \subset C^u_{f(x)}$ and $\|Df_x(\mathbf{v})\| \geq |\lambda^u|\,\|\mathbf{v}\|$
- $Df_x\left(C^s_{f(x)}\right)^{-1} \subset C^s_{f(x)}$ and $\left\|Df^{-1}_{f(x)}(\mathbf{w})\right\| \geq \left|(\lambda^s)^{-1}\right|\|\mathbf{w}\|$

We say that C^s, C^u are stable and unstable cone-fields of f respectively.

Figure 6 illustrates the image $f(\mathcal{R})$ of $\mathcal{R}$ by a *generalized Lozi map* f.

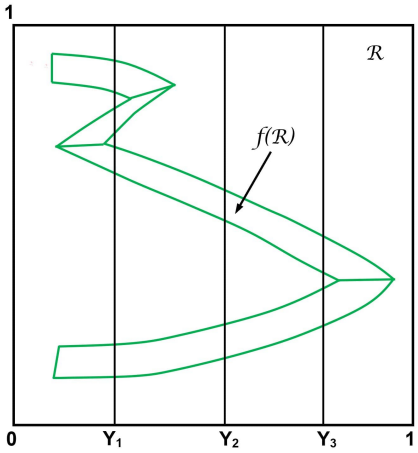

Figure 6. Image $f(\mathcal{R})$ of $\mathcal{R}$ by a *generalized Lozi map* f in the sense of Young [32].

In [32] Lai-Sang Young proves that *Lozi-like maps* have invariant measures with absolutely continuous conditional measures on unstable manifolds. As a consequence they have Bowen-Ruelle measures. More recently Sakurai [35] shows that certain *Lozi-like maps* have the orbit-shifted shadowing property.

Another kind of topological generalization also called *Lozi-like map* was recently introduced by Misiurewicz and Stimac [33]. Its definition is not straightforward and needs some preliminaries.

Definition 1 ([33]). *Let $F_1, F_2 : \mathbb{R}^2 \longrightarrow \mathbb{R}^2$ be C^1 diffeomorphisms. We say that F_1 and F_2 are synchronously hyperbolic if they are either both order reversing, or both order preserving, and there exist $\lambda > 1$, a universal pair of cones K^u and K^s, and cone fields C^u and C^s (consisting of cones K^u_P and K^s_P, $P \in \mathbb{R}^2$, respectively) which satisfy the following properties:*

(S1) For every point $P \in \mathbb{R}^2$ we have $K^u_P \subset K^u$, $K^s_P \subset K^s$, $DF_{iP}(K^u_P) \subset (K^u_{F_{i(P)}})$ and $DF^{-1}_{iP}(K^s_P) \subset (K^s_{F^{-1}_{i(P)}})$, for $i = 1, 2$.

(S2) For every point $P \in \mathbb{R}^2$ and $i = 1, 2$ we have $\|DF_i(\boldsymbol{u})\| \geq \lambda\,\|\boldsymbol{u}\|$ for every $\boldsymbol{u} \in K^u_P$ and $\left\|DF^{-1}_i(\boldsymbol{w})\right\| \geq \lambda\,\|\boldsymbol{w}\|$ for every $w \in K^s_P$.

(S3) There exists a smooth curve $\Gamma \subset \mathbb{R}^2$ such that for every $P \in \Gamma$ we have $F_1(P) = F_2(P)$, the vector tangent to Γ at P belongs to K^s_P, and the vector tangent to $F_i(\Gamma)$ at $F_i(P)$ belongs to $K^u_{F_{i(P)}}$. We require that Γ is infinite in both directions.

We call Γ the *divider*. It divides the plane into two parts which we call the *left half-plane* and the *right half-plane*. Also $F_1(\Gamma) = F_2(\Gamma)$ divides the plane into two parts which we call the *upper half-plane* and the *lower half-plane*.

Definition 2 ([33]). *Let $F_1, F_2 : \mathbb{R}^2 \longrightarrow \mathbb{R}^2$ be synchronously hyperbolic $\mathcal{C}^1$ diffeomorphisms with the divider Γ.*

Preprints (www.preprints.org) | NOT PEER-REVIEWED | Posted: 11 May 2023 doi:10.20944/preprints202305.0775.v1

Let $F : \mathbb{R}^2 \longrightarrow \mathbb{R}^2$ *be defined by the formula:*

$$F(P) = \begin{cases} F_1(P), \text{ if } P \text{ is in the left half-plane,} \\ F_2(P), \text{ if } P \text{ is in the right half-plane,} \end{cases} \tag{11}$$

We call the map F *Lozi-like if the following hold:*

(L′.1) $-1 < det\ DF_i(P) < 0$ *for every point* $P \in \mathbb{R}^2$ *and* $i = 1, 2$.

(L′.2) There exists a trapping region Δ *(for the map* F*), which is homeomorphic to an open disk and its closure is homeomorphic to a closed disk.*

Using these new definition of *Lozi-like map*, Misiurewicz and Stimac [33] show a strong numerical evidence that there exist *Lozi-like maps* that have kneading sequences different than those of Lozi maps.

2.2.2. Geometrical generalization: *Lozi-type map*

Juang and Chang [34] consider a map T of the form

$$T \begin{pmatrix} x \\ y \end{pmatrix} = \begin{pmatrix} y, \\ F(y) - b. \end{pmatrix} \tag{12}$$

If $F(y)$ is a polynomial of degree n with negative leading coefficient and distinct real roots, this map T will henceforth be called an *nth-degree Henon-type* map. If $F(y)$ is replaced by a n-piecewise affine terms, this map T is called an *nth-degree Lozi-type* map (here the term *degree* is given by analogy to polynomial by these authors, however it should be better to use *nth-piecewise*).
This map is defined in relation to a discrete version of a reaction-diffusion system. Juang and Chang consider several spatial entropies, in particular $h(T)$, $h_D(T)$, $h_N(T)$, (spatial entropy with respect to the Dirichlet and Neuman boundary conditions) and other special spatial entropies that they define, and compare them.

2.2.3. Formulas generalization

There are several generalisation of the map $\mathcal{L}_{a,b}$.
In [36] Aiewcharoen et al. say that motivated by (3), they introduce the following system of difference equations:

$$\begin{cases} x_{n+1} = |x_n| - ay_n - b, \\ y_{n+1} = x_n - c\,|y_n| + d, \end{cases} \tag{13}$$

where $b > 4$.
They proof that:

(i) all solutions converge toward the equilibrium point $(-1, -2)$. Moreover, for a large value of x_0 and y_0, they prove that if $b = 5$, then the solution converges toward the equilibrium point $(-1, -3)$ and,
(ii) if $b = 6$, then the solution converges towards the periodic solution of period 5.

A trivial 3-dimensional generalization is proposed by Mammeri and Kina [37] where the stability of its fixed points is investigated.

$$\begin{cases} x_{n+1} = 1 - bz_n + a\,|x_n|\,, \\ y_{n+1} = x_n, \\ z_{n+1} = y_n. \end{cases} \tag{14}$$

Preprints (www.preprints.org) | NOT PEER-REVIEWED | Posted: 11 May 2023 doi:10.20944/preprints202305.0775.v1

Another simple generalization is mentioned in Joshi et al. [38] without analysis. Only a figure in three dimension is plotted in the case $\alpha = 1.7$ and $\overline{\beta} = \beta = 0.08$.

$$\begin{cases} x_{n+1} = 1 - \alpha\,|x_n| + y_n, \\ y_{n+1} = \overline{\beta} y_n, \\ z_{n+1} = 1 - \alpha\,|z_n| + \beta x_n. \end{cases} \tag{15}$$

In Bilal and Ramaswamy [39], the equation corresponding to the map (3) is written as (note the parameter $(1-\nu)$ instead of b)

$$\begin{cases} x_{n+1} = 1 - a\,|x_n| - (1-\nu) y_n, \\ y_{n+1} = x_n. \end{cases} \tag{16}$$

This equation is rewritten as a difference delay equation,

$$x_n = 1 - a\,|x_{n-1}| - (1-\nu) x_{n-2}, \tag{17}$$

which suggests a natural generalization to higher dimensions,

$$x_n = 1 - a\,|x_{n-k}| - (1-\nu) x_{n-d}. \tag{18}$$

Here d and k are integers such that $k < d$, and $0 \leq \nu \leq 2$. The mapping is conservative when ν is 0 or 2 and is dissipative otherwise. For $\nu = 1$, the map reduces to a k-dimensional endomorphism, while for $\nu \neq 1$ the map is a d-dimensional diffeomorphism.

A bifurcation analysis and an investigation of the dynamics through both numerical and analytical is carried out in this article. Moreover a smooth approximation of (18) is obtained replacing the absolute value function $|\cdot|$ with a smooth function $S_\epsilon(\cdot)$:

$$x_n = 1 - a S_\epsilon(x_{n-k}) - (1-\nu) x_{n-d}, \tag{19}$$

$$S_\epsilon(x_{n-k}) = \begin{cases} x_{n-k}^2 \setminus 2\epsilon + \epsilon \setminus 2 & \text{if } |x_{n-k}| \leq \epsilon, \\ |x_{n-k}| & \text{if } |x_{n-k}| \geq \epsilon, \end{cases} \tag{20}$$

where $0 < \epsilon < 1$.

This smooth approximation of the map enables the analysis of the bifurcations vis-a-vis the bifurcations to the generalized the Hénon map. It shows that some of the bifurcations observed persist on both the piecewise Lozi and Hénon map. This kind of smoothing was previously introduced by Lozi [40] in 1979.

This generalized Lozi map (17) is also studied in by Chutani et al. [41] who analyze the time series obtained from different dynamical regimes of evolving maps and flows by constructing their equivalent time series networks, using the visibility algorithm. They focus on the three-dimensional Lozi map (with $d = 3, k = 2$) that displays hyperchaotic dynamical behavior (see Section 3.1) at certain parameter values, in particular at $(a, \nu) = (1.3, 0.6)$.

Another kind of generalization is done by Lopesino et al. [31] who define a *non-autonomous Lozi map* as the map.

$$L_n(x, y) = (1 + y - a(n)\,|x|\,, -x)\,, \tag{21}$$

where $a(n) = a + \epsilon(1 + cos(n))$, $a > 4$. They proof the existence of a chaotic saddle in the square

$$\mathcal{S}_n = \left\{ (x, y) \in \mathbb{R}^2 \mid |x| \leq R,\ |y| \leq R \right\}$$

Preprints (www.preprints.org) | NOT PEER-REVIEWED | Posted: 11 May 2023 doi:10.20944/preprints202305.0775.v1

with

$$R = \sup_{n\in\mathbb{N}} \frac{a(n)}{4(a(n)-2)}$$

(see (10) for comparison).

2.2.4. Fractal mappings

The new paradigm of *fractional mappings* recently explored is a natural extension of the theory of *fractal ordinary differential equations*.

In Khennaoui et al. [42] using the Caputo-like delta difference

$$\begin{aligned} {}^{c}\Delta_a^u X(t) &= \Delta_a^{-(n-\nu)}\Delta^n X(t), \\ &= \frac{1}{\Gamma(n-\nu)}\sum_{s=a}^{t-(n-\nu)}(t-s-1)^{(n-\nu-s)}\Delta^n X(t) \end{aligned}$$

the fractal Lozi map is defined as:

$$\begin{cases} {}^{c}\Delta_a^u x(t) &= \alpha\,|x(t-1+\nu)| + y(t-1+\nu) + 1 - x(t-1+\nu), \\ {}^{c}\Delta_a^u y(t) &= \beta x(t-1+\nu) - y(t-1+\nu), \end{cases} \tag{22}$$

for $0 < \nu \leq 1$ and $t \in \mathbb{N}_{a+1-\nu}$. One can note that the fractional order of both fractional differences are identical leading to what is commonly referred to as a commensurate system. An equivalent discrete integral equation of such a map is obtained:

$$\begin{cases} x(t) &= x(a) + \frac{1}{\Gamma(\nu)}\sum_{s=a+1}^{t-\nu}(t-s-1)^{(\nu-1)}\left(-\alpha\,|x(t-1+\nu)| + y(t-1+\nu) + 1 - x(t-1+\nu)\right), \\ y(t) &= y(a) + \frac{1}{\Gamma(\nu)}\sum_{s=a-\nu}^{t-\nu}(t-s-1)^{(\nu-1)}\left(\beta x(t-1+\nu) - y(t-1+\nu)\right), \end{cases} \tag{23}$$

where $\frac{(t-s-1)^{(\nu-1)}}{\Gamma(\nu)}$ is the discrete kernel function

$$\frac{(t-s-1)^{(\nu-1)}}{\Gamma(\nu)} = \frac{\Gamma(t-s)}{\Gamma(\nu)\Gamma(t-s-\nu+1)},$$

and $a = 0$ yields the numerical formula

$$\begin{cases} x(n) &= x(0) + \frac{1}{\Gamma(\nu)}\sum_{j=1}^{n}\frac{\Gamma(n-j+\nu)}{\Gamma(n-j+1)}\left(-\alpha\,|x(j-1)| + y(j-1) + 1 - x(j-1)\right), \\ y(n) &= y(0) + \frac{1}{\Gamma(\nu)}\sum_{j=1}^{n}\frac{\Gamma(n-j+\nu)}{\Gamma(n-j+1)}\left(\beta x(j-1) - y(j-1)\right). \end{cases} \tag{24}$$

A complete numerical analysis of this fractional map shows that the value of the fractional order ν affects the bifurcation diagram (of the non-fractional map) both in terms of its general shape and the duration of the chaotic interval. For $\nu = 0.98$, the bifurcation diagram is similar to the corresponding integer diagram except for a small broadening in the interval where the chaos is observed. As ν decreases further, it is found that when $0 \leq \alpha \leq 0.5$, the orbit no longer goes to a fixed point. In fact, as n increases, one observes that the trajectory becomes unbounded. A major difference between the bifurcation diagram of the integer and fractional maps is in the interval over which chaos is observed. The interval becomes slightly smaller as ν decreases.

In [43], a combined Hénon-Lozi fractional map is defined and studied.

2.2.5. Non-conventional generalization

A non-conventional generalization of (3) based on the cosine chaotic map has been recently published [44]. Cosine Chaotic Map (CCM) is the chaotification method that enhances the chaotic complexity of the existing chaotic maps. This method performs the cosine function alongside a chaotic map that cascade in used system. So the results provide a new chaotic map having a wide chaotic range

Preprints (www.preprints.org) | NOT PEER-REVIEWED | Posted: 11 May 2023 doi:10.20944/preprints202305.0775.v1

within the closed interval $[-1,+1]$. Theoretically, the CCM has properties based on the properties of the underlying seed maps. In the case of the Lozi map, Aliwi and Ajeena consider (3) changing 1 to 3 in the first component

$$f\begin{pmatrix} x \\ y \end{pmatrix} = \begin{pmatrix} 3 - a\,|x| + y, \\ bx, \end{pmatrix} \tag{25}$$

with $a = -1.8$ and $b = 0.25$. Then they insert (25) in CCM

$$f\begin{pmatrix} x \\ y \end{pmatrix} = \begin{pmatrix} cos\left(2^{(k+3-a|x|+y)}\right), \\ cos\left(2^{(k+bx)}\right), \end{pmatrix} \tag{26}$$

where $k \in [10, 24]$.

Starting with any initial point (x_0, y_0) belonging to the basin of attraction of the Lozi map, the iterates fulfill randomly the square $[-1,+1]^2$ (See Figure 7).

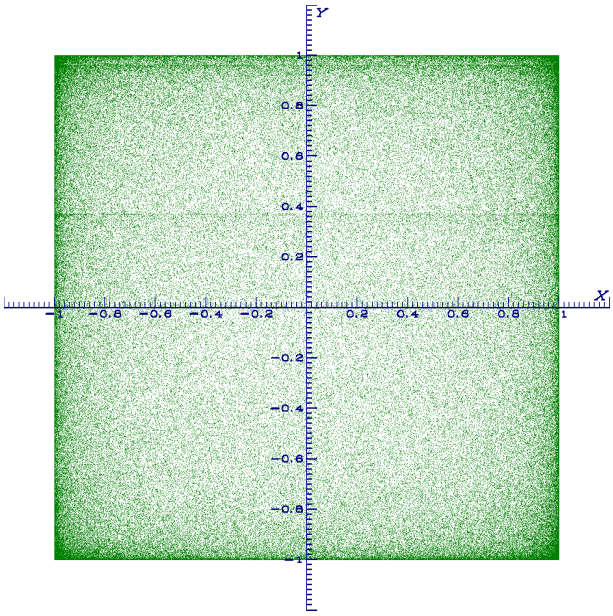

Figure 7. Image on the (x, y)-plane of 300,000 iterates of the cosine Lozi chaotic map [44]. Initial value $(x_0 = 0.1, y_0 = 0.3$.

This generalized map is built for cryptographic purpose. In [45], these authors, for the same purpose combine the Lozi map with the sine function instead:

$$f\begin{pmatrix} x \\ y \end{pmatrix} = \begin{pmatrix} sin\left(2^{(k+3-a|x|+y)}\right), \\ sin\left(2^{(k+bx)}\right). \end{pmatrix} \tag{27}$$

2.2.6. Network of chaotic maps and chimera

Beside the generalizations presented above, the Lozi map can be used to construct networks of chaotic attractors, either alone or with Hénon map.
Cano and Cosenza [46] consider the autonomous system of globally coupled Lozi maps described by the equations

$$\begin{cases} x^i_{n+1} = (1-\epsilon) f(x^i_n, y^i_n) + \epsilon h_n, \\ y^i_{n+1} = b x^i_n, \end{cases} \tag{28}$$

with $f(x_n, y_n) = 1 - a\,|x_n| + y_n$ and $h_n = \frac{1}{N}\sum_{j=1}^{N} f(x^i_n, y^i_n)$.

Preprints (www.preprints.org) | NOT PEER-REVIEWED | Posted: 11 May 2023 doi:10.20944/preprints202305.0775.v1

The parameter ϵ represents the strength of the global coupling of the maps.

Synchronization in this system of equations at the iterate n arises when $(x_n^i, y_n^i) = (x_n^j, y_n^j), \forall (i,j)$. Note that synchronization of the x variable implies synchronization of the y variable. Besides synchronization, the following collective states can be defined in this globally coupled system:

(i) *Clustering*. A dynamical cluster is defined as a subset of elements that are synchronized among themselves. In a clustered state, the elements in the system segregate into K distinct subsets that evolve in time; i.e., $x_n^i = x_n^j = X_n^\nu, \forall (i,j)$ in the υth cluster with $\nu = 1, \ldots, K$

(ii) A *chimera state* consists of the coexistence of one or more clusters and a subset of desynchronized elements.

(iii) A *desynchronized or incoherent state* occurs when $x_n^i \neq x_n^j, \forall (i,j)$.

They consider also the system of nonlocally coupled Lozi maps described by

$$\begin{cases} x_{n+1}^i = (1-\epsilon) f(x_n^i, y_n^i) + \epsilon h_n, \\ y_{n+1}^i = b x_n^i, \end{cases} \tag{29}$$

with

$$h_n^i = \frac{1}{2k} \sum_{j=i-k}^{j=i+k} \left[f(x_n^i, y_n^i) - f(x_n^j, y_n^j) \right], \tag{30}$$

where the elements $i = 1, \ldots, N$ are located on a ring with periodic boundary conditions, ϵ is the coupling parameter, k is the number of neighbors coupled on either side of site i, and h_n^i is the local field acting on element i.

The presence of chimera states in globally coupled networks of identical oscillators seemed at first counterintuitive because of the perfect symmetry of such a system. However, such networks are among the simplest extended systems that can exhibit chimera behavior. Cano and Cosenza highlight that the presence of global interactions can indeed allow for the emergence of chimera states in networks of coupled elements possessing chaotic hyperbolic attractors, such as Lozi maps, where such states do not form with local interactions.

Both chimeras and clusters can be interpreted as manifestations of the multistability of the resulting drive-response dynamics at the local level in systems with global interactions. Their results suggest that chimera states, as other collective behaviors, arise from the interplay between the local dynamics and the network topology; either ingredient can prevent or induce its occurrence.

Semenova et al. [47] study a slighted variant of (29):

$$\begin{cases} x_{n+1}^i = f(x_n^i, y_n^i) + \frac{\sigma 1}{2P} \sum_{j=i-P}^{j=i+P} \left[f(x_n^j, y_n^j) - f(x_n^i, y_n^i) \right], \\ y_{n+1}^i = b x_n^i, \end{cases} \tag{31}$$

$i = 1, 2, \ldots, N$, where N is the number of elements in the ensemble of coupled equations. The nonlocal coupling is characterized by the coupling strength ϵ, the number of neighbours $2P$ (P neighbors on the either side of the ith element), and the coupling range $r = P/N$.

They show that the ensemble of nonlocally coupled Lozi maps demonstrates the solitary state for specific values of coupling parameters. The coupling changes the properties of partial elements, and leads to the bistability, though the Lozi map do not have this property in the uncoupled form. The emergence of solitary states is accompanied by the arising of the second attracting set for the ensemble element.

Others example of chimera states are exhibited by Anishchenko et al. [48] who explore numerically the dynamics of two coupled one-dimensional ensembles: an ensemble of Hénon maps and an ensemble of Lozi maps. Both networks are considered under conditions of non-local coupling. The ensemble of Lozi maps is characterized by a hyperbolic attractor of the individual elements, while the ensemble of Henon maps - by a non-hyperbolic attractor. They reveal the features of realizing

Preprints (www.preprints.org) | NOT PEER-REVIEWED | Posted: 11 May 2023 doi:10.20944/preprints202305.0775.v1

chimera states in the coupled system, which are caused by mutual influence of two ensembles with fundamentally different dynamics without coupling.

3. Three dimensional hyperchaotic attractors

A hyperchaotic attractor of a discrete dynamical system is usualy defined as a chaotic behavior with at least two positive Lyapunov exponents. Combined with one negative exponent to ensure the convergence of the iterates toward the attractor the minimal dimension for a discrete hyperchaotic system is 3. Therefore, for a continuous dynamical system, four ordinary Differential Equations (ODE) are required.

3.1. Rössler hyperchaotic attractors

In 1979, Rössler proposed several examples of systems of four ODE and 3-D mappings providing hyperchaos. Two of them are presented in this section.

3.1.1. The "noodle" attractor

First, in [49]

$$\begin{cases} x_{n+1} = -ax_n(1-x_n^2) - y_n - z_n, \\ y_{n+1} = bx_n, \\ z_{n+1} = c(z_n^2 - 0.33) + dz_n, \end{cases} \tag{32}$$

with $a = 2.7$, $b = 0.09$, $c = 0.09$, and $b = 0.4$.

The projection of this attractor (See Figure 8) onto the (x, y)-plane looks like "folded noodles" as said by Rössler himself, which indicates that this kind of attractor possesses only "one direction of lateral expansion".

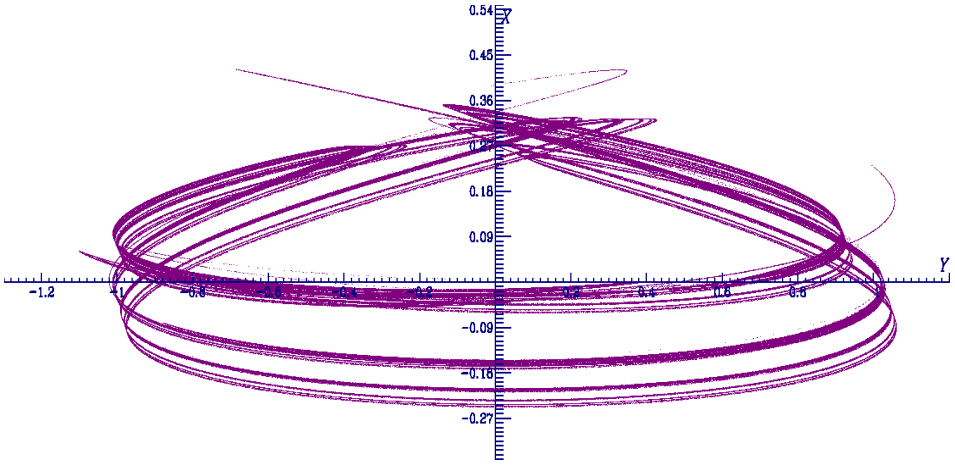

Figure 8. Projection onto the (x, y)-plane of the 3-D Rössler "noodle" hyperchaotic attractor. Initial value ($x_0 = 0$, $y_0 = 0.2$, $z_0 = 0$).

3.1.2. The folded "curtain" attractor

Second, in [50] there is the following

$$\begin{cases} x_{n+1} = 3.4x_n(1-x_n) - 0.05(y_n + 0.35)(1-2z_n), \\ y_{n+1} = 0.1\left[(y_n + 0.35)(1-2z_n) - 1\right](1-1.9x_n), \\ z_{n+1} = 3.78z_n(1-z_n) + 0.01y_n. \end{cases} \tag{33}$$

The projection of this attractor (See Figure 9) onto the (y, x)-plane looks like a folded curtain.

Preprints (www.preprints.org) | NOT PEER-REVIEWED | Posted: 11 May 2023 doi:10.20944/preprints202305.0775.v1

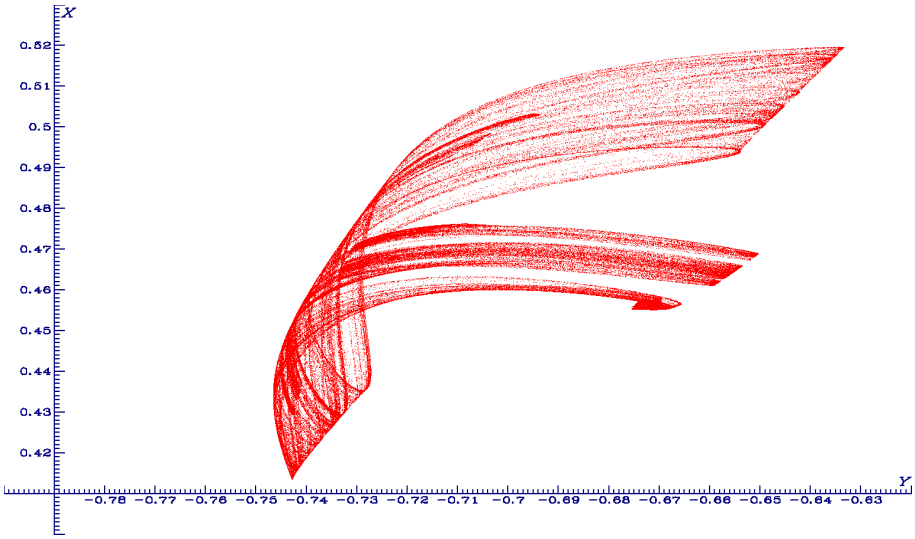

Figure 9. Projection onto the (y, x)-plane of the 3-D Rössler "curtain" hyperchaotic attractor. Initial value ($x_0 = 0.1$, $y_0 = 0.1$, $z_0 = 0.1$).

3.2. 3-Dimensional Lozi map with coexistence of thread and sheet hyperchaotic attractor

The most important features of the classical Lozi map $\mathcal{L}_{a,b}$ (3), are its simplicity and piecewise linearity which makes formal calculus easily tractable. The previous examples of Rössler (32) and (33), both with a third order nonlinearity and with five and nine parameters cannot be analyzed analytically nor thoroughly by numerical computation. It is why, in this section, one introduces a much simpler example of hyperchaos, based on the use of piecewise linearity. Moreover, one wants to conserve another essential feature of the Lozi map: the determinant of the Jacobian matrix ought to be constant. This is a tough condition which implies to define a not continuous mapping. However there are several advantages to keep such determinant constant like assuming hyperbolicity.

As pointed out in [17], in 2-Dimension the main advantage of the Lozi map over the Hénon map is that one can prove hyperbolicity without much effort. This is the main reason why so little is known for the Hénon map, where hyperbolicity is believed to occur only on Cantor-like sets of parameters. The Lozi map is rather similar to Sinai's billiards, in particular, the discontinuity of the differential allows the uniform hyperbolicity as in the billiards case. The uniformly hyperbolic attractors were introduced in mathematical theory on dynamical systems due to Smale, Anosov, Sinai, and other researchers in the 1960s-1970s [51]. Hyperbolic attractors are characterized by roughness or structural stability. In the context of physical or technical objects it implies insensitivity of the dynamical behavior to small variations in parameters, manufacturing imperfections, interferences, etc. that may be significant for possible applications [52]. It turned out, however, that hyperbolic chaos is not widespread in real-world systems, and its implementation requires special efforts [53].

Hence, the proposed *thread-sheet* hyperchaotic attractor is:

$$\begin{cases} x_{n+1} = a\,|x_n| + y_n\, sgn(z_n) + 1, \\ y_{n+1} = b(x_n + z_n), \\ z_{n+1} = y_n\, sgn(x_n) + c\,|z_n| + 1, \end{cases} \tag{34}$$

also represented by the iterates of any initial point $(x_0, y_0, z_0)^T$ by the map $T_{a,b,c} : \mathbb{R}^3 \longrightarrow \mathbb{R}^3$:

$$T_{a,b,c} \begin{pmatrix} x \\ y \\ z \end{pmatrix} = \begin{pmatrix} a\,|x| + y\, sgn(z) + 1, \\ b(x + z), \\ y\, sgn(x) + c\,|z| + 1, \end{pmatrix} \tag{35}$$

Preprints (www.preprints.org) | NOT PEER-REVIEWED | Posted: 11 May 2023 doi:10.20944/preprints202305.0775.v1

with $sgn(x) = 1$ if $x \geq 0$, and $sgn(x) = -1$ if $x < 0$. The particularity of this map is that one can observe for many values of the parameters (when $a = c$), coexistence of two chaotic attractors having different dimensionality: a *thread*-strange attractor which belongs to the plane (x, z) and a *sheet*-strange attractor with a three-dimensional structure. This *thread*-chaotic attractor is a combination of straight lines, instead the *sheet*-chaotic attractor seems made of a bunch of planes (See Figures 10 and 11).

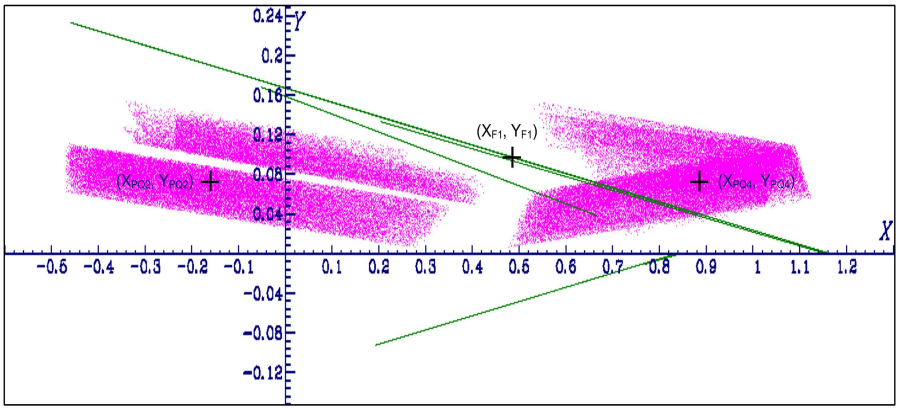

Figure 10. Projection onto the (x, y)-plane of the coexisting *sheet* and *thread* 3-D Lozi map hyperchaotic attractors for the parameter value $a = -1.25, b = 0.1, c = -1.25$. Initial value of the *thread*-attractor (in green) ($x_0 = 0.1$, $y_0 = 0.2$, $z_0 = 0.1$). Initial value of the *sheet*-attractor (in purple) ($x_0 = 0.11$, $y_0 = 0.2$, $z_0 = 0.1$).

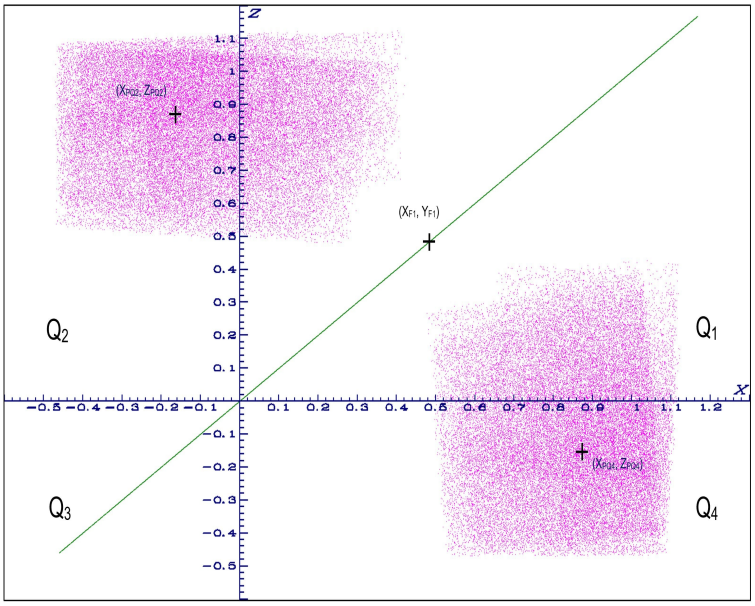

Figure 11. Projection onto the (x, z)-plane of the coexisting *sheet* and *thread* 3-D Lozi map hyperchaotic attractors for the parameter value $a = -1.25, b = 0.1, c = -1.25$. Initial value of the *thread*-attractor (in green) ($x_0 = 0.1$, $y_0 = 0.2$, $z_0 = 0.1$). Initial value of the *sheet*-attractor (in purple) ($x_0 = 0.11$, $y_0 = 0.2$, $z_0 = 0.1$).

One cand find some analogy in dimensionality between the *thread*-chaotic attractor and the "noodle attractor"proposed by Rössler (32), on one hand, and on the other hand between the *sheet*-chaotic attractor and its folded "curtain" chaotic attractor (33).

In this article, we keep the name *sheet*-chaotic attractor even if its structure is more complicated (See Figures 12 and 13).

Preprints (www.preprints.org) | NOT PEER-REVIEWED | Posted: 11 May 2023 doi:10.20944/preprints202305.0775.v1

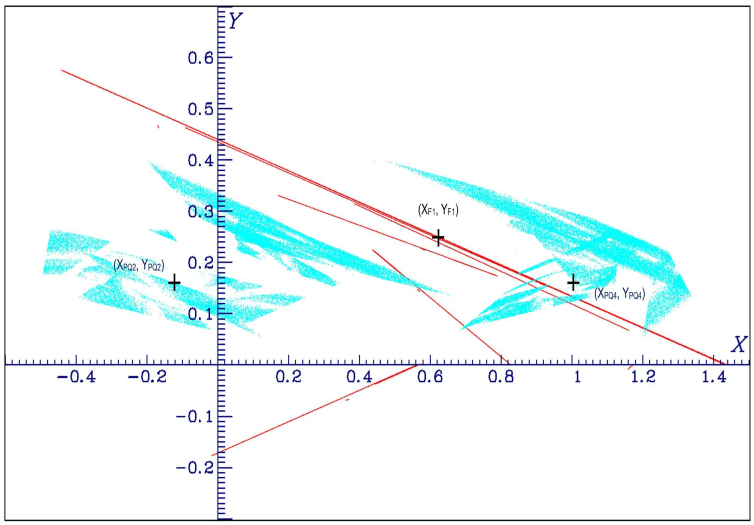

Figure 12. Projection onto the (x, y)-plane of the coexisting *sheet* and *thread* 3-D Lozi map hyperchaotic attractors for the parameter value $a = -1.0, b = 0.2, c = -1.0$, initial value of the *thread*-attractor (in red) ($x_0 = 0.1$, $y_0 = 0.2$, $z_0 = 0.1$). Initial value of the *sheet*-attractor (in cyan) ($x_0 = 0.11$, $y_0 = 0.2$, $z_0 = 0.1$).

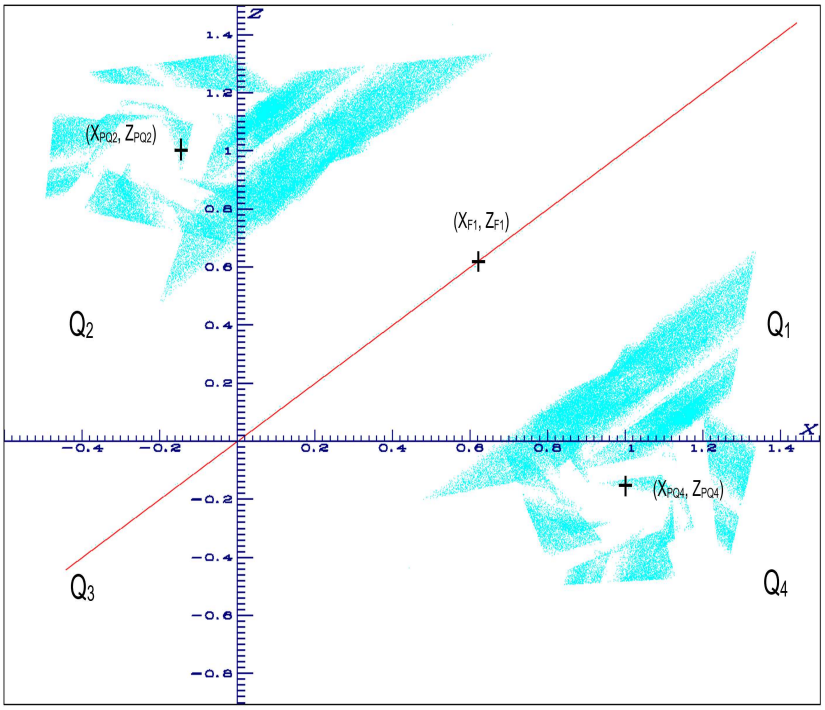

Figure 13. Projection onto the (x, z)-plane of the coexisting *sheet* and *thread* 3-D Lozi map hyperchaotic attractors for the parameter value $a = -1.0, b = 0.2, c = -1.0$, initial value of the *thread*-attractor (in red) ($x_0 = 0.1$, $y_0 = 0.2$, $z_0 = 0.1$). Initial value of the *sheet*-attractor (in cyan) ($x_0 = 0.11$, $y_0 = 0.2$, $z_0 = 0.1$).

4. Properties of thread-sheet hyperchaotic attractor

In this section, some properties of $T_{a,b,c}$ the are given. Even if the piecewise linear functions composing this map allow to perform explicit calculations, there is a need of a huge amount of studies to completely understand its dynamics. One can compare this situation with the studies on Lozi map for which 46 years after its discovery, important features are still discovered (see for example the Ph. Thesis of Kilassa Kvaternik [54] defensed in 2022 on the tangential homoclinic points locus of $\mathcal{L}_{a,b}$).

Preprints (www.preprints.org) | NOT PEER-REVIEWED | Posted: 11 May 2023 doi:10.20944/preprints202305.0775.v1

4.1. Basic properties: jacobian and symmetry

The map $T_{a,b,c}$ (35) is much simpler than the hyperchaotic maps proposed by Rössler (32) and (33). It is also different from generalizations of Lozi map described in Section 2.2.3. For convenience, henceforth the following notation of $T_{a,b,c}$ is used

$$T_{a,b,c}\begin{pmatrix} x \\ y \\ z \end{pmatrix} = \begin{pmatrix} a_X x + 1_Z y + 1, \\ b(x+z), \\ 1_X y + c_Z z + 1, \end{pmatrix} \tag{36}$$

with $a_X = asgn(x)$, $c_Z = csgn(z)$ (because $a_X x = a\,|x|$ and $c_Z z = c\,|z|$), $1_X = sgn(x)$ and $1_Z = sgn(z)$.

If $x \neq 0$ and $z \neq 0$, the jacobian matrix $J_{a,b,c}$ of $T_{a,b,c}$ is definite

$$J_{a,b,c}\begin{pmatrix} x \\ y \\ z \end{pmatrix} = \begin{pmatrix} a_X & 1_Z & 0 \\ b & 0 & b \\ 0 & 1_X & c_Z \end{pmatrix} \tag{37}$$

and, as $1_X a_X = a$ and $1_Z c_Z = c$ its determinant is

$$\text{Det } J_{a,b,c} = -b(a+c).$$

Therefore, the map is dissipative and can have an attractor if and only if $-1 < -b(a+c) < 1$.

It is interesting to note that there is a symmetry conjugating parameters and variables

$$T_{a,b,c}(x,y,z) = T_{c,b,a}(z,y,x). \tag{38}$$

4.2. The thread attractor

If $a = c$ there is a special projection of (36) in the plane $(x = z, y)$ which reduces the map $T_{a,b,c}$ to $T_{a,b}$

$$T_{a,b}\begin{pmatrix} x \\ y \end{pmatrix} = \begin{pmatrix} a_X x + 1_X y + 1, \\ 2bx. \end{pmatrix} \tag{39}$$

This map as a 2-D chaotic attractor which is the thread attractor observed in Figures 10–13. Its structure is fractal as shown in Figure 14.

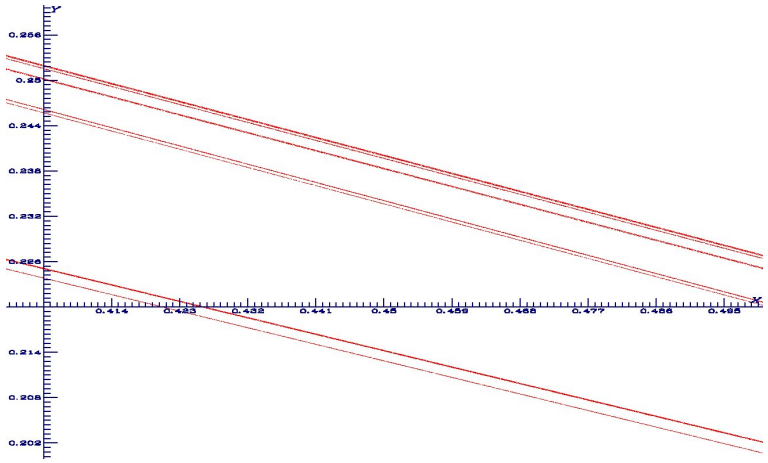

Figure 14. Magnification of Figure 10 on the $(x = z, y)$-plane of the *thread*-attractor, showing its fractal structure. Parameter value $a = -1.0, b = 0.2, c = -1.0$, initial value of the *thread*-attractor ($x_0 = 0.1$, $y_0 = 0.2$, $z_0 = 0.1$).

Preprints (www.preprints.org) | NOT PEER-REVIEWED | Posted: 11 May 2023 doi:10.20944/preprints202305.0775.v1

4.3. Fixed points and period-two orbits

As seen in Section 2.1.3, fixed points play an important role shaping the chaotic attractors and their basin of attraction. In the following, the plane (x, z) is divided in four quadrants: $Q_1 = \{x \geq 0,\ z \geq 0\}$, $Q_2 = \{x < 0,\ z \geq 0\}$, $Q_3 = \{x < 0,\ z < 0\}$, $Q_4 = \{x \geq 0,\ z < 0\}$.

The fixed points of $T_{a,b,c}$ are obtained solving the system

$$T_{a,b,c} \begin{pmatrix} x \\ y \\ z \end{pmatrix} = \begin{pmatrix} x \\ y \\ z \end{pmatrix} \tag{40}$$

whose solutions are:

$$\begin{cases} x_F = \frac{1-c_{Z_F}-b_{X_F}+b_{Z_F}}{\Delta}, \\ y_F = \frac{b(2-a_{X_F}-c_{Z_F})}{\Delta}, \\ z_F = \frac{1-a_{X_F}-b_{Z_F}+b_{X_F}}{\Delta}, \end{cases} \tag{41}$$

where

$$\Delta = a_{X_F} c_{Z_F} + b(a - 1_{Z_F} - 1_{X_F} + c) + 1 - c_{Z_F} - a_{X_F}\ ,$$

with $b_{X_F} = b1_{X_F}$, $b_{Z_F} = b1_{Z_F}$, provided the sign of x_F and z_F are in accordance with those of the coefficients in the quadrant where the solution belongs (see example below and in Section 4.4). This implies that there can exist at most (but not always) four fixed points (one in each quadrant) instead of only two for the 2D-Lozi map.

The related eigenvalue of the Jacobian are the roots of the characteristic polynomial

$$P(\lambda) = -\lambda^3 + \lambda^2(a_X + c_Z) + \lambda\left(b(1_X + 1_Z)a_X c_Z\right) - b(a + c). \tag{42}$$

As an example the fixed point in the quadrant Q_1 is

$$\begin{cases} x_{F_1} = \frac{1-c}{\Delta}, \\ y_{F_1} = \frac{b(2-a-c)}{\Delta}, \\ z_{F_1} = \frac{1-a}{\Delta}, \end{cases} \tag{43}$$

with $\Delta = ac + b(a + c - 2) + 1 - c - a$, because $1_{X_{F_1}} = 1 = 1_{Z_{F_1}}$, and $b_{X_{F_1}} = b = b_{Z_{F_1}}$.

For some parameter values like those of Figures 10–13, it seems that the chaotic attractor is generated by the unstable invariant manifold of a period-two orbit belonging to Q_4 and Q_2. The piecewise linear form of (36) allows to compute the periodic orbit of any period. In the case of period-two with $(x_{PQ_2}, z_{PQ_2}) \in Q_2$ and $(x_{PQ_4}, z_{PQ_4}) \in Q_4$, the value of $(x_{PQ_4}, y_{PQ_4}, z_{PQ_4})$ is obtained solving the system

$$\begin{cases} (-a^2 + b - 1)x_{PQ_4} + a y_{PQ_4} + b z_{PQ_4} = a - 1, \\ abx_{PQ_4} - y_{PQ_4} - bcz_{PQ_4} = -2b, \\ bx_{PQ_4} - cy_{PQ_4} + (b + c^2 + 1)z_{PQ_4} = c + 1 \end{cases} \tag{44}$$

which gives the solution

$$\begin{cases} x_{PQ_4} = \frac{a-2ab^2-ab-2b+ac^2-bc^2-c^2-2b^2c+abc-bc-1}{\Delta}, \\ y_{PQ_4} = \frac{-a^2b^2-2ab^2-ab^2-ab-2b+b^2c^2-abc^2-bc^2-2b^2c+a^2bc+bc}{\Delta}, \\ z_{PQ_4} = \frac{-a^2+2ab^2+a^2b-ab+2b-a^2c+2bc^2-abc-bc-c-1}{\Delta} \end{cases} \tag{45}$$

Preprints (www.preprints.org) | NOT PEER-REVIEWED | Posted: 11 May 2023 doi:10.20944/preprints202305.0775.v1

with $\Delta = b^2(a+c)^2 - (a^2+c^2+a^2c^2) - 1$, provided that $\Delta \neq 0$ and the condition $(x_{PQ_4}, z_{PQ_4}) \in Q_4$ depending on the parameter values is verified. Then

$$x_{PQ_2} = z_{PQ_4},\ y_{PQ_2} = y_{PQ_4},\ z_{PQ_2} = x_{PQ_4}.$$

4.4. Numerical examples

This new 3-dimensional mapping can generate a large variety of chaotic and hyperchaotic attractors. We give five examples of such behavior in this section. In the first three examples, there is coexistence of *thread* and *sheet* chaotic attractors. However, their shape are different and they are constituted by a different number of pieces. In the two last examples, the blow up of the attractors with respect to parameter a and b is highlighted.

4.4.1. Case a=-1.25, b=0.1, c=-1.25, one piece chaotic attractor, two-pieces hyperchaotic attractor

The value of the Jacobian is 0.25. In this case, there exist four fixed points, two of them are in the plane $(x = z, y)$ and are related to the *thread*-attractor.

In Q_1, the fixed point belongs to the plane $x = z$ (see Figures 10 and 11):

$$x_{F_1} = z_{F_1} = 20/41 \approx 0.487804,\ y_{F_1} = 4/41 \approx 0.097560,$$

The corresponding eigenvalues of the Jacobian matrix are

$$\lambda_1 \approx -1.393521, \lambda_2 = -1.25, \lambda_3 \approx +0.143521,$$

Hence the dimension of the unstable invariant manifold in $\mathbb{R}^3$ of this fixed point $(x_{F_1}, y_{F_1}, z_{F_1})$ is two (and those of the stable invariant manifold is one). However, in the plane $(x = z, y)$ the map $T_{a,b}$ (39) has only two eigenvalues

$$\lambda_1 \approx -1.393521, \lambda_2 = +0.143521.$$

Therefore in this plane the unstable invariant manifold of the fixed point (x_{F_1}, y_{F_1}) is only 1-dimensional, like the stable invariant manifold. This unstable invariant manifold nests the skeleton of the *thread*-chaotic attractor (see Figure 10).

In Q_3, the fixed point belongs also to the plane $x = z$:

$$x_{F_3} = z_{F_3} = -20,\ y_{F_3} = -4.$$

The corresponding eigenvalues of the Jacobian matrix are

$$\lambda_1 \approx +1.06161, \lambda_2 = +1.25, \lambda_3 \approx +0.188394,$$

Hence the dimension of the unstable invariant manifold in $\mathbb{R}^3$ of this fixed point $(x_{F_1}, y_{F_1}, z_{F_1})$ is two (and those of the stable invariant manifold is one). However, in the plane $(x = z, y)$ the map $T_{a,b}$ (39) has only two eigenvalues

$$\lambda_1 \approx +1.06161, \lambda_2 = +0.188394.$$

Therefore in this plane the unstable invariant manifold of the fixed point (x_{F_3}, y_{F_3}) is only 1-dimensional, like the stable invariant manifold. In analogy with the results displayed in Section 2.1.3, it is reasonable to think that the invariant stable manifold of (x_{F_3}, y_{F_3}) allows to define the boundary of the basin of attraction of the *thread*-attractor. However this point remains to proof, (see for example in Figure 1.2 of [54] the complicated shape of the stable and unstable manifold of the unstable fixed point of $\mathcal{L}_{a,b}$ for the values $a = 1.46$, $b = 0.86$).

Preprints (www.preprints.org) | NOT PEER-REVIEWED | Posted: 11 May 2023 doi:10.20944/preprints202305.0775.v1

The other two fixed points (x_{F_2}, y_{F_2}) and (x_{F_4}, y_{F_4}), belong to Q_2 and Q_4.

$$x_{F_2} = \frac{-2.45}{0.8125} \approx -3.015385,\ y_{F_2} = \frac{-0.2}{0.8125} \approx -0.246154,\ z_{F_2} = \frac{0.45}{0.8125} \approx 0.553846,$$

and

$$x_{F_4} = \frac{0.45}{0.8125} \approx 0.553846,\ y_{F_4} = \frac{-0.2}{0.8125} \approx -0.246154,\ z_{F_4} = \frac{-2.45}{0.8125} \approx -3.015385.$$

One can remark the symmetry:

$$x_{F_2} = z_{F_4},\ y_{F_2} = y_{F_4},\ z_{F_2} = x_{F_4},$$

The corresponding eigenvalues of the Jacobian matrix of these fixed point $(x_{F_2}, y_{F_2}, z_{F_2})$ and $(x_{F_4}, y_{F_4}, z_{F_4})$ are

$$\lambda_1 \approx +1.32341, \lambda_2 = +0.162759, \lambda_3 \approx -1.16065.$$

There also exists a period-two orbit of the type discussed in the previous section

$$x_{PQ_4} = \frac{196}{225} \approx 0.87111,\ y_{PQ_4} = \frac{16}{225} \approx 0.071111, z_{PQ_4} = \frac{-4}{225} = -0.16;$$

$$x_{PQ_2} = z_{PQ_4},\ y_{PQ_2} = y_{PQ_4},\ z_{PQ_2} = x_{PQ_4}.$$

It seems that each piece of this *sheet*-hyperchaotic attractor is linked to one component of the period-two orbit (see Figures 10 and 11).

Moreover, there does not exist period-two orbit going from Q_1 to Q_3 and vice-versa.

4.4.2. Case a=-1.0, b=0.2, c=-1.0, multi-pieces chaotic and hyperchaotic attractor

The value of the Jacobian is 0.4. In this case, there exist only three fixed points, one of them is in the plane $(x = z, y)$ and is related to the *thread*-attractor (see Figures 12 and 13).

$$x_{F_1} = z_{F_1} = 5/8 = 0.625,\ y_{F_1} = 1/4 = 0.25.$$

The eigenvalues of the Jacobian matrix are

$$\lambda_1 \approx -1.306226, \lambda_2 = -1.0, \lambda_3 \approx +0.306226,$$

Hence the dimension of the unstable invariant manifold of this fixed point is one (and those of the stable invariant manifold is one). However, in the plane $(x = z, y)$ the map (39) has only two eigenvalues

$$\lambda_1 \approx -1.306226, \lambda_2 = +0.306226,$$

Therefore in this plane the unstable invariant manifold of this fixed point is only 1-dimensional like for the stable manifold. This unstable invariant manifold is the skeleton of the *thread*-attractor (see Figure 12).

However, in Q_3, there is no fixed point. Therefore the boundary of the basin of attraction of the thread chaotic attractor cannot be linked to a second fixed point in the plane.

The other two fixed points (x_{F_2}, y_{F_2}) and (x_{F_4}, y_{F_4}), belong to Q_2 and Q_4.

$$x_{F_2} = -6,\ y_{F_2} = -1,\ z_{F_2} = 1,$$

and

$$x_{F_4} = 1,\ y_{F_4} = -1,\ z_{F_4} = -6.$$

Preprints (www.preprints.org) | NOT PEER-REVIEWED | Posted: 11 May 2023 doi:10.20944/preprints202305.0775.v1

One can remark again the symmetry:

$$x_{F_2} = z_{F_4},\ y_{F_2} = y_{F_4},\ z_{F_2} = x_{F_4},$$

There also exists a period-two orbit of the type discussed in the previous section

$$x_{PQ_4} = 1,\ y_{PQ_4} = 1/6 \approx 0.16666, z_{PQ_4} = -1/6 \approx -0.16666;$$

$$x_{PQ_2} = z_{PQ_4},\ y_{PQ_2} = y_{PQ_4},\ z_{PQ_2} = x_{PQ_4},$$

In this case the geometry of the multi-piece hypechaotic attractor is more complicated that those of the previous case, even if the period-two orbit belongs to it (see Figures 12 and 13).

4.4.3. Case a=-1.25, b=0.2, c=-1.25, connected hyperchaotic attractor

The value of the Jacobian is 0.5. In this case, there exist only three fixed points, one of them is in the plane $(x = z, y)$ and is related to the *thread*-attractor (See Figures 15 and 16).

$$x_F = 20/37 \approx 0.54054 = z_F,\ y_F = 8/37 \approx 0.21622.$$

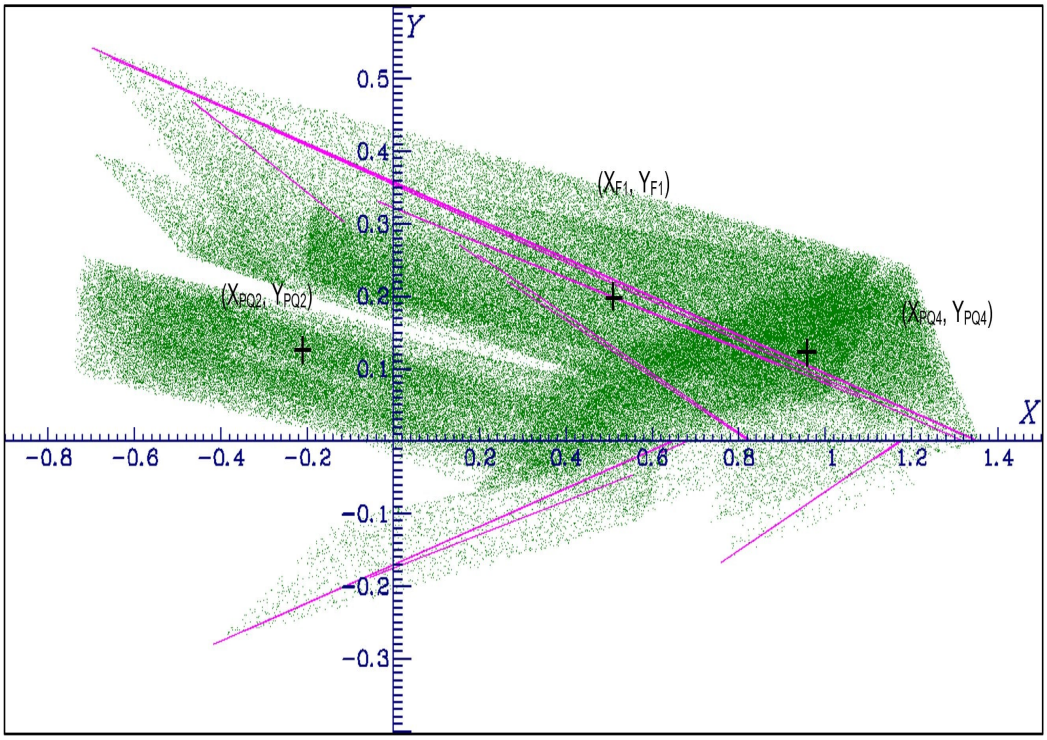

Figure 15. Projection onto the (x, y)-plane of the coexisting *sheet* and *thread* 3-D Lozi map hyperchaotic attractor for the parameter value $a = -1.25, b = 0.2, c = -1.25$. Initial value of the *thread*-attractor (in purple) ($x_0 = 0.1$, $y_0 = 0.1$, $z_0 = 0.1$). Initial value of the *sheet*-attractor (in green) ($x_0 = 0.1$, $y_0 = 0.2$, $z_0 = 0.1$).

Preprints (www.preprints.org) | NOT PEER-REVIEWED | Posted: 11 May 2023 doi:10.20944/preprints202305.0775.v1

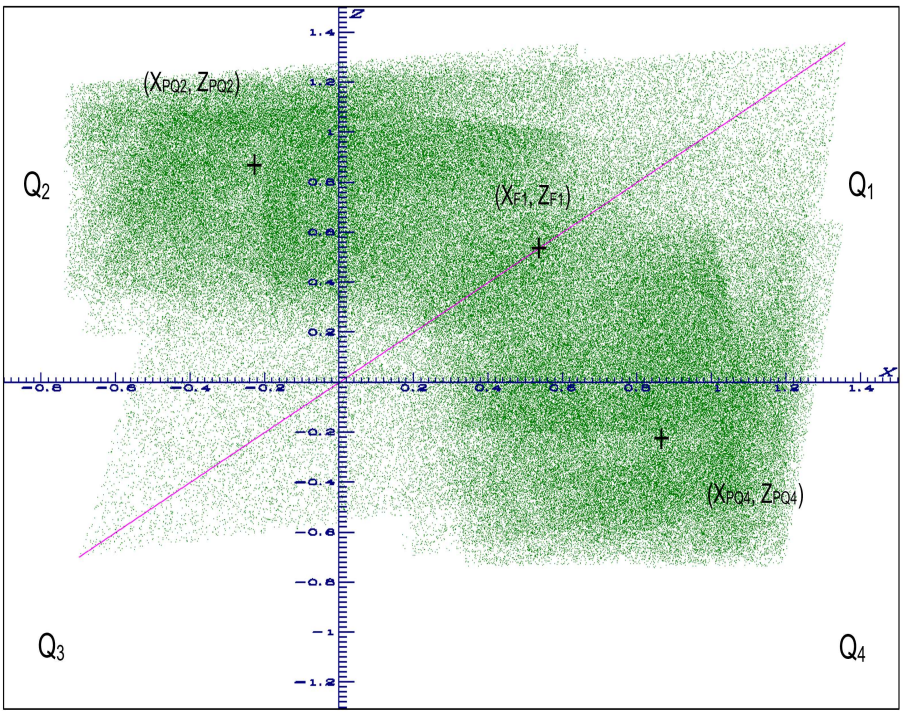

Figure 16. Projection onto the (x, z)-plane of the coexisting *sheet* and *thread* 3-D Lozi map hyperchaotic attractor for the parameter value $a = -1.25, b = 0.2, c = -1.25$. Initial value of the *thread*-attractor (in purple) ($x_0 = 0.125$, $y_0 = 0.2$, $z_0 = 0.125$). Initial value of the *sheet*-attractor (green) ($x_0 = 0.1$, $y_0 = 0.2$, $z_0 = 0.1$).

The eigenvalues of the Jacobian matrix are

$$\lambda_1 \approx -1.514171, \lambda_2 = -1.25, \lambda_3 \approx +0.264171,$$

Hence the dimension of the unstable invariant manifold of this fixed point is two (and those of the stable invariant manifold is one). However, in the plane $(x = z, y)$ the map (39) has only two eigenvalues

$$\lambda_1 \approx -1.514171, \lambda_2 = +0.264171,$$

therefore in this plane the unstable invariant manifold of this fixed point is only 1-dimensional. This unstable invariant manifold is the skeleton of the *thread*-attractor.

However, in Q_3, there is no fixed point.

The other two fixed points (x_{F_2}, y_{F_2}) and (x_{F_4}, y_{F_4}), belong to Q_2 and Q_4.

$$x_{F_2} = \frac{-2.65}{1.0625} \approx -2.49412,\ y_{F_2} = \frac{-0.4}{1.0625} \approx -0.376471,\ z_{F_2} = \frac{0.65}{1.0625} \approx 0.611765,$$

and

$$x_{F_4} = \frac{0.65}{1.0625} \approx 0.611765,\ y_{F_4} = \frac{-0.24}{1.0625} \approx -0.376471,\ z_{F_4} = \frac{-2.65}{1.0625} \approx -2.49412.$$

with again the symmetry

$$x_{F_2} = z_{F_4},\ y_{F_2} = y_{F_4},\ z_{F_2} = x_{F_4}.$$

There also exists a period-two orbit of the type discussed in the previous section

$$x_{PQ_4} = \frac{212}{245} \approx 0.86531,\ y_{PQ_4} = \frac{32}{245} \approx 0.13061, z_{PQ_4} = \frac{-52}{245} = -0.21224;$$

Preprints (www.preprints.org) | NOT PEER-REVIEWED | Posted: 11 May 2023 doi:10.20944/preprints202305.0775.v1

$$x_{PQ_2} = z_{PQ_4},\ y_{PQ_2} = y_{PQ_4},\ z_{PQ_2} = x_{PQ_4}.$$

This case is similar to the first case, however the two components of the *sheet*-hyperchaotic attractor have merged (see Figures 15 and 16).

4.4.4. Case a=-1.365 and a=-1.369, b=0.36, c=0.6, blow up of the attractor versus the parameter a

In this example, the rich dynamics of (36) is highlighted by an example where a very small change of 2‰in the value of a leads to a blow up of the chaotic attractor (see Figures 17 and 18). When $a = -1.365$ (resp. $a = -1.369$) the Jacobian worths 0.27576 (resp. 0.27684).

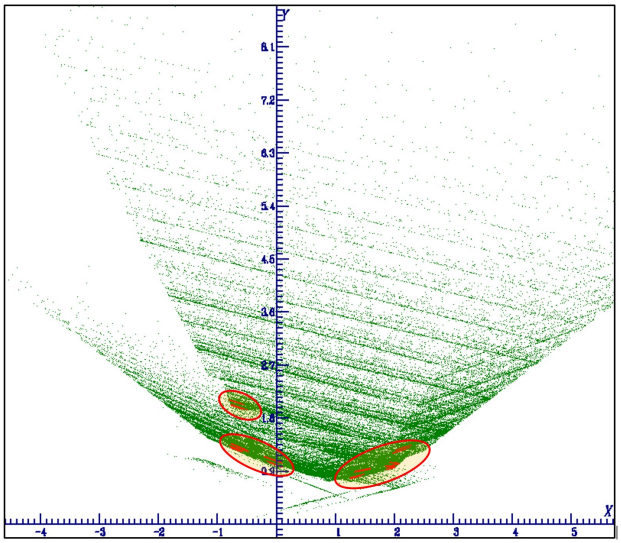

Figure 17. Projection onto the (x, y)-plane of two attractors of the 3-D Lozi map chaotic attractor for the parameter values $a = -1.365$ and $a = -1.369$, $b = 0.36, c = 0.6$. Initial value of both attractors $(x_0 = 0.2, y_0 = 0.1, z_0 = 0.0)$. When $a = -1.365$ the attractor consists in small red lines (in the three oval regions surrounded by a red curve), instead when $a = -1.369$ there is a blow up of the green attractor which is partially displayed in this magnification of the (x, y)-phase plane.

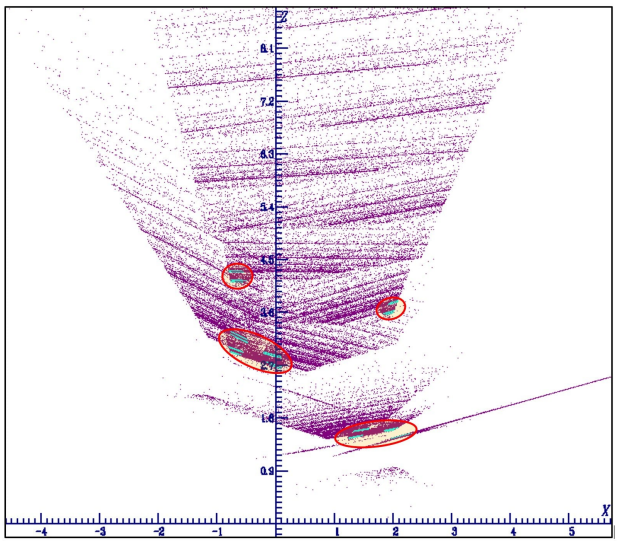

Figure 18. Projection onto the (x, z)-plane of two attractors of the 3-D Lozi map chaotic attractor for the parameter values $a = -1.365$ and $a = -1.369$, $b = 0.36, c = 0.6$. Initial value of both attractors the $(x_0 = 0.2, y_0 = 0.1, z_0 = 0.0)$. When $a = -1.365$ the attractor consists in small cyan lines (in the four oval regions surrounded by a red curve), instead when $a = -1.369$ there is a blow up of the purple attractor which is partially displayed in this magnification of the (x, z)-phase plane.

Preprints (www.preprints.org) | NOT PEER-REVIEWED | Posted: 11 May 2023 doi:10.20944/preprints202305.0775.v1

4.4.5. Case a=-1.369, b=0.02 to b=0.36, c=0.6, blow up of the attractor versus the parameter b

In this example, several values of the parameter b with the same value of $a = -1.369$ leads to a blowing of the size of the chaotic attractor (see Figures 19 and 20). When $b = 0.02$ the Jacobian worths 0.01538; for $b = 0.05$ the Jacobian worths 0.03845; for $b = 0.09$ the Jacobian worths 0.06921, and for $b = 0.16$ the Jacobian worths 0.12304.

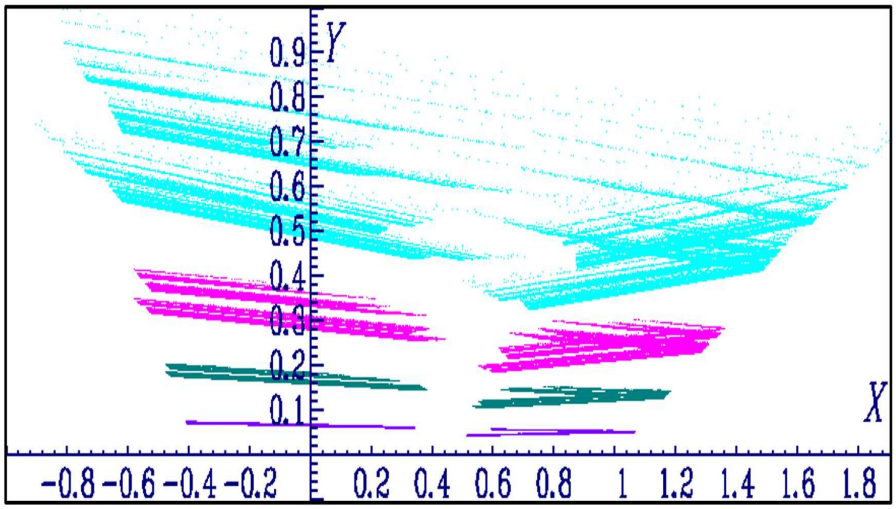

Figure 19. Projection onto the (x, y)-plane of two attractors of the 3-D Lozi map chaotic attractor for the parameter values $a = -1.369$, $c = 0.6$, $b = 0.02$ (violet), $b = 0.05$ (blue), $b = 0.09$ (purple) and $b = 0.16$ (cyan). Initial value for all attractors ($x_0 = 0.2$, $y_0 = 0.1$, $z_0 = 0.0$). The attractors for each value of b remain in a small bounded region of the (x, y)-plane. When b is increased more (see next figure), there is a blowing of the size of the attractor, which remains bounded however.

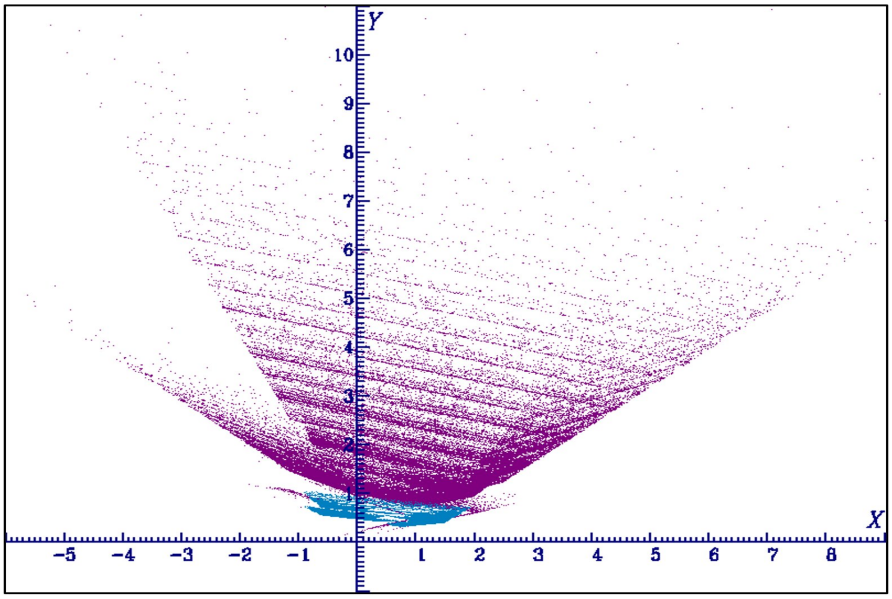

Figure 20. Continuation of the previous figure. Projection onto the (x, y)-plane of two attractors of the 3-D Lozi map chaotic attractor for the parameter values $a = -1.369$, $c = 0.6$, $b = 0.16$, (cyan) and $b = 0.36$ (purple). Initial value of both attractors ($x_0 = 0.2$, $y_0 = 0.1$, $z_0 = 0.0$). When $b = -0.16$ the attractor has a small size, instead when $a = 0.36$ there is a blow up of the purple attractor which is partially displayed in this magnification of the (x, y)-phase plane.

5. Conclusion

In this article a three-dimensional piece-wise linear extension of the two-dimensional Lozi map is introduced which respects the constraint of a constant Jacobian. It displays a special property never highlighted for chaotic mappings: the coexistence of *thread*-chaotic attractors (i.e., attractors which are formed by collection of lines) and *sheet*-hyperchaotic attractors (i.e., attractors which are formed by collection of planes). This new 3-dimensional mapping can generate a large variety of chaotic and hyperchaotic attractors. Five prototypical examples of such behavior are gieven. In the first three examples, there is coexistence of *thread* and *sheet*-chaotic attractors. However, their shape are different and they are constituted by a different number of pieces. In the two last examples, the blow up of the attractors with respect to parameter a and b is highlighted.

References

1. Zeraoulia, E. *Lozi mappings — Theory and applications*; CRC Press: Boca Raton, London, New York, 2013; 309p.
2. Letellier, C.; Abraham, R.; Shepelyansky, D. L.; Rössler, O. E.; Holmes, P.; Lozi, R.; Glass, L.; Pikovsky, A.; Olsen, L.F.; Tsuda, I.; Grebogi, C.;Parlitz, U.; Gilmore, R.; Pecora, L. M.; Carroll, T. L. Some elements for a history of the dynamical systems theory. *Chaos* **2021**, *Vol. 31*, 053110. doi:10.1063/5.0047851
3. Ruelle, D. Dynamical systems with turbulent behavior. In *Mathematical Problems in Theoretical Physics*, *Lecture Notes in Physics*, edited by G. Dell'Antonio et al. (Springer, 1978), *Vol. 80*, pp. 341–360; International Mathematics Physics Conference, Roma, 1977. doi:10.1007/3-540-08853-9_28
4. Lorenz, E. N. Deterministic nonperiodic flow. *Journal of the Atmospheric Sciences* **1963**, *Vol. 20*, pp. 130–141. doi:10.1175/1520-0469(1963)020<0130:DNF>2.0.CO;2
5. Hénon, M. A two-dimensional mapping with a strange attractor. *Commun. Math. Phys.* **1976**, *Vol. 50*, pp. 69–77. doi:10.1007/BF01608556
6. Smale, S. Differentiable dynamical systems. I Diffeormorphisms. *Bulletin of American Mathematical Society* **1967**, *vol. 73*, pp. 747–817. doi:10.1007/978-1-4613-8101-3_1
7. Lozi, R. Un attracteur étrange (?) du type attracteur de Hénon. *Journal de Physique* **1978**, *vol. 39*, C5–9–C5–10. doi:10.1051/jphyscol:1978505
8. Misiurewicz, M. Strange attractors for the Lozi mappings. *Annals of the New York Academy of Sciences* **1980**, *vol. 357*, pp. 348–358. doi:10.1111/j.1749-6632.1980.tb29702.x
9. Misiurewicz, M.; Stimac, S. Symbolic dynamics for Lozi maps. *Nonlinearity* **2016**, *vol. 29* pp. 3031-3046 doi:10.1088/0951-7715/29/10/3031
10. Kucharski, P. Strange attractors for the family of orientation preserving Lozi Maps. https://arxiv.org/pdf/2211.10296.pdf **2022**
11. Baptista, D.; Severino, R.; Vinagre, S. The basin of attraction of Lozi Mappings. *International Journal of Bifurcation and Chaos* **2009**.*vol. 19, No. 3*, pp. 1043-1049. doi:10.1142/S0218127421300469
12. Ishii, Y. Towards a kneading theory for Lozi mappings I: A solution of the pruning front conjecture and the first tangency problem. *Nonlinearity* **1997** *vol. 10 , no. 3*, pp. 731-747. doi:10.1088/0951-7715/10/3/008
13. Boroński, J.P.; Kucharski, P.; Ou, D.-S. Lozi maps with periodic points of all periods n > 13. Preprint. https://www.researchgate.net/publication/366740872_Lozi_maps_with_periodic_points_of_all_periods_n_13 **2022**
14. Botella-Soler, V.; Castelo, J. M.; Oteo, J. A.; Ros, J. Bifurcations in the Lozi map. *J. Phys. A: Math.Theor.* **2011**, *vol. 44, no. 30*, p. 305101. doi:10.1088/1751-8113/44/30/305101
15. Sushko, I.; Avrutin, V.; Gardini, L. Center Bifurcation in the Lozi Map. *International Journal of Bifurcation and Chaos* **2021**.*vol. 31, No. 16*, p. 2130046. doi:10.1142/S0218127421300469
16. Glendinning, P.A.; Simpson, D.J.W. Chaos in the border-collision normal form: A computer-assisted proof using induced maps and invariant expanding cones. *Applied Mathematics and Computation* **2022** , *vol. 434*, p. 127357. doi:10.1016/j.amc.2022.127357

17. Collet, P.; Levy, Y. Ergodic properties of the Lozi mappings. *Commun. Math. Phys.* **1984**, *vol. 93*, pp. 461–482. doi:10.1007/BF01212290
18. Rychlik, M. Invariant Measures and the Variational Principle for Lozi Mappings. In: Hunt, B.R., Li, TY., Kennedy, J.A., Nusse, H.E. (eds) *The Theory of Chaotic Attractors* **2004**. Springer, New York, NY. doi:10.1007/978-0-387-21830-4_13
19. Cao, Y.; Liu, Z. The Geometric Structure of Strange Attractors in the Lozi Map. *Communications in Nonlinear Science and Numerical Simulation* **1998**, *vol. 3, Iss. 2*, pp. 119-123. doi:10.1016/S1007-5704(98)90076-4
20. Afraimovich, V. S.; Chernov, N. I.; Sataev, E. A. Statistical properties of 2-D generalized hyperbolic attractors. *Chaos* **1995** *vol. 5*, pp. 238-252. doi:10.1063/1.166073
21. Zheng W.-M. Symbolic Dynamics for the Lozi Map. *Chaos. Solitons & fractals* **1991** *vol. 1, No 3*, pp. 243-248. doi:10.1016/0960-0779(91)90034-7
22. Ishii, Y. Towards a kneading theory for Lozi mappings II: Monotonicity of the Topological Entropy and Hausdorff Dimension of Attractors. *Communications in Mathematical Physics* **1997** ,*vol. 190* , pp. 375–394. doi:10.1007/s002200050245
23. Ishii, Y.; Sands. D. Monotonicity of the Lozi family near the tent-maps. *Comm. Math. Phys.* **1998**, *Vol. 198(2)* pp.397-406. doi:10.1007/s002200050482
24. Carvalho (de), A.; Hall, T. How to prune a horseshoe. *Nonlinearity* **2002**, *Vol. 15* pp. R19-R68. doi:10.1088/0951-7715/15/3/201
25. Li, H.; Li, K.; Chen, M.; Bao, B. Coexisting Infinite Orbits in an Area-Preserving Lozi Map. *Entropy* **2020**, *vol. 22* , pp. 1119. doi:10.3390/e22101119
26. Natiq, H.; Banerjee, S.; Ariffin, M.R.K.; Said, M.R.M. Can hyperchaotic maps with high complexity produce multistability? *Chaos* **2019**, *vol. 29* , pp. 011103. doi:/10.1063/1.5079886
27. Zhusubaliyev, Z.T.; Mosekilde, E. Multistability and hidden attractors in a multilevel DC/DC converter. *Math. Comput. Simul.* **2015**, *vol. 109*, pp. 32–45. doi:10.1016/j.matcom.2014.08.001
28. Bao, B.C.; Li, H.Z.; Zhu, L.; Zhang, X.; Chen, M. Initial-switched boosting bifurcations in 2D hyperchaotic map. *Chaos* **2020**, *vol.30*, p. 033107. doi: DOI: 10.1063/5.0002554
29. Zhang, L.-P.; Liu, Y.; Wei, Z.-C.; Jiang, H.-B.; Bi, Q.-S. A novel class of two-dimensional chaotic maps with infinitely many coexisting attractors. *Chin. Phys. B* **2020**, *vol.29*, p. 060501. doi:10.1088/1674-1056/ab8626
30. Bao, H.; Hua, Z.Y.; Wang, N.; Zhu, L.; Chen, M.; Bao, B.C. Initials-boosted coexisting chaos in a 2D Sine map and its hardware implementation. *IEEE Trans. Ind. Inform.* **2021**, *vol.17, Iss. 2*, pp. 1132 - 1140. doi:10.1109/TII.2020.2992438
31. Lopesino, C.; Balibrea, F.; Wiggins, S. R.; Mancho, A. M. The Chaotic Saddle in the Lozi Map, Autonomous and Nonautonomous Versions. I*nternational Journal of Bifurcation and Chaos* **2015**, *vol. 25, no. 13*, p.1550184. doi:10.1142/S0218127415501849
32. Young, L.-S. A Bowen-Ruelle measure for certain piecewise hyperbolic maps. *Trans. Amer. Math. Soc.* **1985**, *Vol. 287*, pp. 41-48.
33. Misiurewicz, M.; Stimac, S. Lozi-like maps. *Discrete and Continuous Dynamical Systems* **2018**, *Vol. 38(6)*, pp. 2965-2985. doi:10.3934/dcds.2018127
34. Juang , J.; Chang, Y.-C. Boundary influence on the entropy of a Lozi-type map. *J. Math. Anal. Appl.* **2010** *vol. 371* , pp. 728-740. doi:10.1016/j.jmaa.2010.06.004
35. Sakurai, A. Orbit shifted shadowing property of generalized Lozi map. *Taiwanese Journal of Mathematics* **2010**, *Vol. 14*, No. 4 pp. 1609-1621 https://www.jstor.org/stable/43834956
36. Aiewcharoen, B.; Boonklurb, R.; Konglawan, N. Global and Local Behavior of the System of Piecewise Linear Difference Equations $x_{n+1} = |x_n| - y_n - b$ and $y_{n+1} = x_n - |y_n| + 1$ Where $b \geq 4$. *Mathematics* **2021**, *vol. 9*, 1390. doi:10.3390/math9121390
37. Mammeri, M.; Kina, N. E. Dynamical properties of solutions in a 3-D Lozi map. Proceedings of the 6th International Arab Conference on Mathematics and Computations (IACMC2019), Aliaa Burqan, Osama Ababneh and Shawkat Alkhazaleh (eds.), Zarqa University, Jordan, pp.27-33.
38. Joshi, Y.; Blackmore, D.; Rahman, A. Generalized Attracting Horseshoes and Chaotic Strange Attractors. doi:10.48550/arXiv.1611.04133.v2
39. Bilal, S.; Ramaswamy, R. A higher-dimensional generalization of the Lozi map: bifurcations and dynamics. *J. Difference Equations and Applications* **2022**, 12 p. doi:10.1080/10236198.2022.2041625

40. Lozi, R. Strange attractors: a class of mapping of R2 which leaves some Cantor sets invariant. In *Intrinsic stochasticity in plasmas*, **1979** Laval, G.; Gresillon, D. (eds.), Cargese, 17-23 June 1979, Les Editions de Physique, Orsay, France, pp. 373-381.
41. Chutani, M.; Rao, N.; Nirmal Thyagu, N.; Gupte, N. Characterizing the complexity of time series networks of dynamical systems: A simplicial approach. *Chaos* **2020** *vol. 30*, p. 013109 (2020). doi:10.1063/1.5100362
42. Khennaoui A.-A.; Ouannas, A.; Bendoukha, S.; Grassi, G.; Lozi, R.; Pham, V.-T. On fractional–order discrete-time systems: Chaos, stabilization and synchronization. *Chaos, Solitons and Fractals* **2019**, *vol.119*, pp. 150-162. doi:10.1016/j.chaos.2018.12.019
43. Ibrahim, R. W.; Baleanu, D. Global stability of local fractional Hénon-Lozi map using fixed point theory. *AIMS Mathematics* **2022**, *Vol. 7(6)*, pp. 11399–11416. doi:10.3934/math.2022636
44. Aliwi, B. H.; Ajeena, R. K. K. A performed knapsack problem on the fuzzy chaos cryptosystem with cosine Lozi chaotic map. *AIP Conference Proceedings* **2023**, *vol. 2414,*, pp. 040047. doi:10.1063/5.0114840
45. Aliwi, B. H.; Ajeena, R. K. K. On Fuzzy Sine Chaotic Based Model in Security Communications. *Journal of Positive School Psychology* **2022**, *Vol. 6, No. 4*, pp. 8127 – 8133. https://journalppw.com/index.php/jpsp/article/view/5169
46. Cano, A. V.; Cosenza, M. G. Chimeras and clusters in networks of hyperbolic chaotic oscillators. *Phys. Rev. E* **2017**, *Vol. 95*, pp. 030202(R). doi:10.1103/PhysRevE.95.030202
47. Semenova, N.; Vadivasova, T.; Anishchenko, V. Mechanism of solitary state appearance in an ensemble of nonlocally coupled Lozi maps. *Eur. Phys. J. Special Topics* **2018** , *Vol. 227*, pp.1173-1183. doi:10.1140/epjst/e2018-800035-y
48. Anishchenko, V.; Rybalova, E.; Semenova, N. Chimera States in two coupled ensembles of Henon and Lozi maps. Controlling chimera states. *AIP Conference Proceedings* **2018**, *Vol. 1978*, pp. 470013-1–470013-4. doi:10.1063/1.5044083
49. Rössler, O. E.; Hudson, J. L.; Farmer, J. D. Noodle-map chaos: a simple example. In: Schuster, P. (eds) *Stochastic Phenomena and Chaotic Behaviour in Complex Systems*. Springer Series in Synergetics, **1984**,*vol 21*. Springer, Berlin, Heidelberg. doi:10.1007/978-3-642-69591-9_5
50. Rössler, O. E. An equation for hyperchaos. *Physics Letters* **1979**, *Vol. 71A*, no 2-3, pp. 155-157. doi:10.1016/0375-9601(79)90150-6
51. Anosov, D.V. et al. *Dynamical Systems IX: Dynamical Systems with Hyperbolic Behaviour* **1995**, (*Encyclopedia of Mathematical Sciences: Vol. 9*), Springer. doi:10.1007/978-3-662-03172-8
52. Elhadj, Z.; Sprott, J. C. *Robust Chaos and Its Applications* **2011**, Singapore: World Scientific Series on Nonlinear Science Series A: Volume 79. doi:10.1142/8296
53. Kuznetsov, S. P. Some lattice models with hyperbolic chaotic attractors. *Russian Journal of Nonlinear Dynamics* **2020**, *Vol. 16, No 1*, pp. 13–21. doi:10.20537/nd200102
54. Kilassa Kvaternik, K. Tangential homoclinic points locus of the Lozi maps. *Doctoral thesis* **2022**, University of Zagreb, 110 p. https://repozitorij.pmf.unizg.hr/islandora/object/pmf:11546